UNIVERSIDADE DO ALGARVE

FACULDADE DE ENGENHARIA DE RECURSOS NATURAIS

Functional Characterisation of Novel Neuropeptides in Vertebrates

Carina Isabel Mascarenhas do Nascimento Cabrita

MESTRADO INTEGRADO DE ENGENHARIA BIOLÓGICA

2009

UNIVERSIDADE DO ALGARVE

FACULDADE DE ENGENHARIA DE RECURSOS NATURAIS

Functional Characterisation of Novel Neuropeptides in Vertebrates

Carina Isabel Mascarenhas do Nascimento Cabrita

MESTRADO INTEGRADO DE ENGENHARIA BIOLÓGICA

Dissertação orientada por: Professora Doutora Deborah Power

Doutor João Cardoso

2009

Preface

The following report is the result of my dissertation to obtain the degree of Master of Biology Engineering from the University of Algarve. This research took place in the FCMA labs within the CCMAR group. During this dissertation I improved my theoretical and practical knowledge in molecular biology and in classical histology techniques.

In this research I used *Xenopus laevis* dorsal skin to evaluate the UV-B induced response and appraised the possible role of certain genes on this response. This work is the beginning of a very important study that will allow accessing the function PTH transcripts and their possible role in skin proliferation and differentiation.

First of all, I would like to thank Professor Deborah Power for the opportunity to work within the CCMAR group and for the challenge that she gave me. I particularly appreciate her guidance when performing histology assays, a new technique for me.

Also, I would like to show my gratitude to my practical supervisor Doctor João Cardoso for his helpful suggestions on this report and also for his support and guidance during the practical work.

Finally, I also would like to thank all other members of the group that created a good work environment, the technician Elsa, Ana, Luiz and Vanessa, the students Silvia, Eduarda, Alexandra, Ângela, Vera, Edison, João, Cristina, Rita and Nadia and the Ph.D. students, Laurence, Florbela, Rita, Patricia, Nicolay, Bruno, Pedro and Pedro Pinheiro.

Carina Isabel Cabrita

March 2009

Abbreviations

aa – Amino acids

AC – Adenyl Cyclase

bp – Base pares

BLAST – Basic Local Alignment Search Tool

CT – Calcitonin

cDNA – Complementary DNA

DEPC – Diethylpyrocarbonate

DMSO – Dimethyl sulfoxide

DNA – Deoxyribonucleic Acid

dNTP – Deoxyribonucleotide Triphosphate

ER – Endoplasmic reticulum

EST – Expressed Sequence Tags

GPCRs – G - Protein Coupled Receptors

HHM – Humoral Hypercalcemia of Malignancy

IHC – Immunohistochemical

IP3 – Inositophospate

IPTG – Isopropyl-D-tiogalactopyranoside

kb – Kilobases

kD – KiloDalton

NCBI – National Center for Biotechnology Information

NLS – Nuclear Localisation Signal

M-MLV – Moloney Murine Leukemia Virus

mRNA – Messenger RNA

O/N – Overnight

PBS – Phosphate Buffer Solution

PCR – Polymerase Chain Reaction

PFA – Paraformaldehyde

Pre-ProPTH – Precursor of ProPTH

ProPTH – Precursor of PTH

PTH – Parathyroid Hormone

PTH-L – Parathyroid Hormone-like Peptide

PTHnR – Parathyroid Hormone Receptor (n = 1, 2 or 3)

PTHrP – Parathyroid Hormone-related Peptide

RACE - Rapid Amplification of cDNA Ends

RNA – Ribonucleic Acid

RNase – Ribonuclease

RT – Room Temperature

RT-PCR – Reverse transcriptase PCR

SP – Signal Peptide

Taq – *Thermus aquaticus*

TIP39 – 39 amino acids of Tuberoinfundibular Peptide

Tm – Melting Temperature

TM – Transmembrane

Top10F' – *Escherichia coli* Top10F'

UTR – Untranslated Regions

UV – Ultraviolet Light

UV-B – Ultraviolet Light-B

X-Gal – 5-bromo-4-chloride-3-indolyl-D-galactopyranoside

XL1_B – *Escherichia coli* XL1-Blue

Abstract

PTH/PTHrP family in vertebrates is composed of three calciotropic hormones: PTH, PTHrP and PTH-L. Three receptors from family 2 GPCRs bind these hormones: PTH1R, PTH2R and PTH3R. PTH is produced by human parathyroid. PTHrP is associated with skin cell carcinomas and might have a role in cell proliferation and differentiation. PTH-L is a recently identified member of this family and little information is available about this peptide. The aim of this study was to estimate possible roles of PTH/PTHrP family on cell proliferation, apoptosis and skin recovery after UV-B exposure. In skin, UV radiation has a variety of carcinogenesis associated effects inducing a response characterized by the modulation of processes such as inflammation, cell proliferation and apoptosis. In this study pigmented and albino *Xenopus laevis* dorsal skin was exposed to UV-B radiation. UV response was evaluated using classical histology and molecular approaches. An UV-B irradiation of 6 J/cm^2 induced apoptosis of keratinocytes within epidermis supra-basal layers of pigmented *Xenopus laevis*. Albino Xenopus laevis dorsal skin was exposed to a lesser UV-B radiation (4.8 J/cm^2) and significant reorganization of skin structure related to culture time was observed. Three biological markers of UV-B response were used to evaluate expression changes (keratin 8, collagen type XVIII and p51/p63). UV-B radiation used significantly modified the expression of all used markers. The evaluation of p51/p63 gene expression was not conclusive in regards to cell apoptosis and another type of tests would be needed (e. g. DNA damage). PTH/PTHrP family member's expression changes due to UV-B exposure were also evaluated. PTH-L expression was maintained constant and does not appear to have a role in UV-B response. Differing, PTHrPA isoform expression increases upon UV-B exposure which might indicate a role in UV response possibly related with cell apoptosis. This work has given some perception on *Xenopus skin* structural and molecular alterations due to UV-B exposure.

Key-words:

Parathyroid Hormone (PTH), Parathyroid-related Peptide (PTHrP), PTH/PTHrP family, *Xenopus*, UV-B response, Skin

Sumário

A família de péptidos PTH/PTHrP possui um papel de vital importância na regulação endócrina do cálcio. A esta família pertencem três hormonas com a mesma função calciotrópica: a hormona da paratiróide (PTH), a proteína relacionada com a PTH (PTHrP) e a *Parathyroid Hormone-like Peptide* (PTH-L). Em humanos, a PTH é produzida na paratiróide. A PTHrP é o factor humoral que provoca a hipercalcemia humoral maligna, sendo a sua produção associada a certos tipos de cancro em humanos, como por exemplo o Carcinoma Espinocelular. Ao contrário do que acontece com a PTH, a PTHrP é expressa em quase todos os tecidos até hoje avaliados e foram descritas múltiplas funções para a mesma. Este facto suscitou o aparecimento de questões relacionadas com a origem e função deste péptido ao longo da evolução. O mais recente membro da família PTH/PTHrP, a PTH-L, foi encontrado em teleósteos, em galinha e em *Xenopus laevis*. A PTH-L é, assim como a PTHrP, expressa em diversos tecidos no entanto, até hoje, apenas foi descrita para este péptido a sua função na regulação do cálcio.

Actualmente são conhecidos três receptores específicos da família 2 dos GPCRs, aos quais as hormonas da família PTH/PTHrP se conseguem ligar: PTH1R, PTH2R e PTH3R. O PTH1R desempenha um papel crucial na regulação endócrina do cálcio e está consequentemente envolvido na formação e desenvolvimento do esqueleto. As funções dos receptores PTH2R e PTH3R ainda não estão discernidas. Os três receptores foram já identificados em *Xenopus laevi*s por Gomes (2007).

A radiação ultravioleta é assumida, na actualidade, como a principal causa de cancro de pele e devido à ligação de um dos membros da família PTH/PTHrP com a carcinógenese da pele é pertinente descortinar o possível papel desta família na resposta aos raios UV. A resposta aos raios UV é caracterizada pela regulação de diversos processos, como por exemplo a inflamação, proliferação celular e apoptose, que permitem evitar danos patológicos definitivos induzidos pelas radiações. O objectivo deste estudo foi avaliar qual o possível papel da família PTH/PTHrP na proliferação celular e recuperação da pele após exposição aos raios ultravioleta-B (UV-B).

Neste trabalho foi utilizado como modelo fisiológico a espécie *Xenopus laevis*. Foram primeiramente usados extractos de pele dorsal de um indivíduo *Xenopus laevis* pigmentado, para avaliar, por histologia clássica, as alterações estruturais induzidas pela exposição aos raios ultravioleta. A pele foi exposta a uma radiação de 6 J/cm^2 durante 5 min e as amostras foram recolhidas em períodos regulares de tempo. Neste estudo pode observar-se que a exposição a raios ultravioleta induziu a apoptose de vários queratinócitos das camadas supra-basais da epiderme dos sapos pigmentados, com grandes alterações a ocorrerem entre as 2 h e as 4 h.

Finalmente, realizou-se uma experiência em que foram usados três grupos de estudo: Grupo A (pele normal), Grupo B (pele mantida em cultura 4 h) e Grupo C (pele exposta a UV-B e mantida em cultura 4 h). Esta experiência final foi realizada com *Xenopus laevis* albino e devido a esse facto reduziu-se ligeiramente a exposição para 4,8 J/cm^2. As alterações estruturais foram avaliadas por histologia clássica, e alterações a nível molecular foram avaliadas usando três marcadores biológicos cuja expressão se altera com a exposição a raios UV. Os marcadores usados foram a queratina 8 para alterações na epiderme, colagénio (tipo XVIII) para modificações na derme e um marcador da apoptose, o gene p51/p63.

Observou-se nos grupos B e C uma desorganização da estrutura da derme e do conteúdo granular, não sendo possível distinguir, através de histologia, diferenças entre os grupos B e C. Deste modo concluiu-se que o tempo em cultura provocou as modificações estruturais observadas. A avaliação dos três marcadores biológicos revelou, no entanto, diferenças significativas entre os grupos B e C, permitindo concluir que a apoptose ocorreu nos extractos expostos a UV-B. Em relação aos membros da família PTH/PTHrP, somente a expressão de dois membros pôde ser avaliada: a PTH-L e a isoforma PTHrPA. A expressão da hormona PTH-L manteve-se constante após exposição a radiação UV-B. Observou-se um aumento da expressão da isoforma PTHrPA induzido pela exposição aos UV-B. Deste modo, a isoforma PTHrPA parece desempenhar um papel na resposta induzida pelo UV-B, nomeadamente, na apoptose.

Palavras-chave:
Hormona da Paratiróide (PTH), Proteína relacionada com a PTH (PTHrP), UV-B, *Xenopus laevis*, pele

List of Contents

1. Introduction

The PTH/PTHrP system has an extreme importance in the endocrine regulation of calcium in vertebrates (Clemens, *et al*., 2001; Guerreiro, *et al*., 2007). PTH/PTHrP systems include three peptides: Parathyroid hormone (PTH), Parathyroid Hormone-related Peptide (PTHrP) and the recently identified PTH-like peptide (PTH-L). Whilst PTH function continue mainly associated with calcium regulation, PTHrP seems to have a pleotropic role and to a great extent its functions remains to be determined (Ingleton, 2002). Moreover, PTHrP is the humoral factor of Humoral Hypercalcemia of Malignancy (HHM) which provokes squamous cell carcinoma in skin (Moseley, *et al*., 1987). PTHrP and PTH are known to activate specific receptors, members of G-Protein Coupled Receptors 2 family (GPCRs), which have been identified in several vertebrates and invertebrates (Harmar, 2001; Kroeze, *et al*., 2003).

In skin, PTHrP seems to be involved in keratinocyte differentiation and proliferation (Merendino, *et al*., 1986) however the mechanisms that are involved on its regulation and what are its functions in skin remain poorly understood. Therefore, the aim of the present study is to further explore the role of the PTH/PTHrP system in the vertebrate skin cell proliferation and recovery using as a model *Xenopus* dorsal explants under ultraviolet light-B (UV-B) exposure. The *Xenopus* skin is an established classical physiological model and PTH/PTHrP system have been previously described in this species (Gomes, 2007) where the homologues of the teleost PTH transcripts and three receptors were characterised. From these, PTHrPB isoform and PTH1R were found to be expressed in skin (Gomes, 2007) although their functional role remains to be established.

1.1 PTH/PTHrP family members

PTH/PTHrP family members have been isolated in several vertebrates and two genes are present in humans: PTH and PTHrP (Bergwitz, *et al*., 1998). In teleosts, amphibians and chicken a novel peptide (PTH-L) exists and it seems to share intermediate PTH and PTHrP characteristics however to date very little is known about its functions (Guerreiro, *et al*., 2007; Canario, *et al*., 2006; Gomes, 2007). The members of the PTH/PTHrP family share at least 70% homology in nucleotide and amino acid sequences for the N-terminal region and in addition they also have similar intron-exon

structural organization. In general, all the members of this family seem to have calciotropic functions by activating specific receptor members of family 2 GPCRs. These receptors have been isolated and characterised from several vertebrates (Harmar, 2001).

1.1.1 PTH and PTHrP gene structure

In human, PTH and PTHrP are products of separate genes: the PTHrP gene (15 kb) is located on the short arm of the chromosome 12 (Mangin, *et al*., 1989) and the PTH gene maps for the short arm of the chromosome 11 (Comings, 1972). The PTH gene structure is maintained constant in the so far studied vertebrates, however PTHrP varies in other vertebrates with a coding region generally more simple (Ingleton, 2002). In human, PTH gene encodes for only one protein whilst PTHrP gene encodes through different promoters for three isoforms with distinct sizes: 139, 141 and 173 aa long (Abbink and Flik, 2006; Philbrick, et al., 1996). Also, in human the gene encoding PTHrP is more complex than the PTH gene (Figure 1.1); the PTHrP gene is composed of nine exons, with the coding sequence for the active hormone located partly on exon 5 and 6 for the 139 aa isoform, on exon 5, 6 and 8 for the 173 aa isoform and on exon 5, 6 and 9 for the 141 aa isoform exon 3 and the pre-pro sequence is located partly on exons 4 and 5; the PTH gene has only three exons with the coding sequence located in exon 2 and 3 and the pre-pro sequence in the exon 1 and 2 (Ingleton, 2002; Clemens, *et al*., 2001).

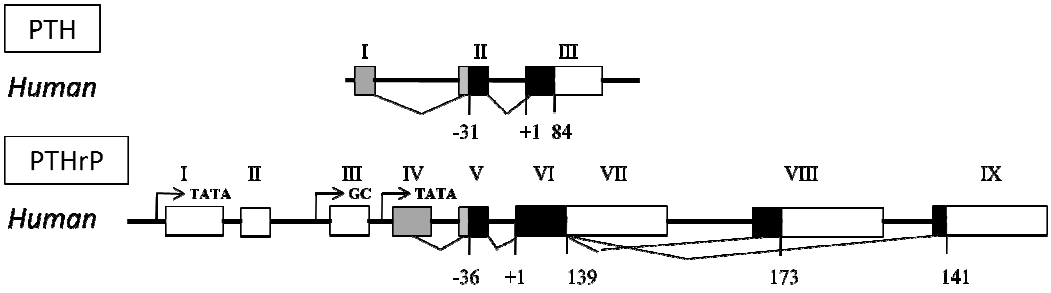

Figure 1.1 – PTH and PTHrP gene organisation in human. The PTH gene with a less complex organization has 3 exons whilst PTHrP presents 9 exons. In white are presented the untranslated regions (UTR), in grey is presented the pre-pro sequence and in black are presented the mature coding regions. The presence of TATA boxes and GC sequences in the promoting region suggest complex regulation of expression of PTHrP (□: exon ─: intron) (adapted from Ingleton, 2002 and Clemens, *et al*., 2001).

1.1.2 PTH and PTHrP regulation

In human, PTH is produced by parathyroid glands in response to low calcium levels in blood and it is initially diffused throughout the body by nearby capillaries (Seeley, *et al*., 2003). The parathyroid gland cells located on the posterior side of the thyroid gland monitor extracellular free calcium concentrations via a membrane calcium-sensing receptor (Campbell and Reece, 2005). PTHrP appears to have a widespread expression in human and a similar pattern is also observed in other vertebrates (Ingleton, 2002; Power, *et al*., 2000).Unlike PTH, the human PTHrP secretion acts in a paracrine/autocrine fashion during foetal and adult life in a number of tissues, including epithelia, mesenchymal tissues, endocrine glands and the central nervous system (Danks, *et al*., 2003; Abbink and Flik, 2006; Philbrick, *et al*., 1996).

The mammalian PTH was the first member of the PTH/PTHrP family to be described and consists of a single polypeptide chain with 84 amino acids (aa) with a molecular weight of approximately 9,4 kD (Habener, *et al*., 1976). The synthesis of the PTH in humans was described by Habener (1976) (Figure 1.2). Initially, an early biosynthetic precursor of PTH is synthesized by parathyroid cells. This precursor, named pre-proparathyroid hormone (Pre-ProPTH) is a 155 aa polypeptide containing the sequence of the intermediate proparathyroid (ProPTH) with a 25 aa sequence linked to the N-terminus (Heinrich, *et al*., 1984). The Pre-ProPTH is synthesized in the cytoplasm on the ribosome attached to the rough endoplasmic reticulum (ER) and is converted by proteolytic cleavage into ProPTH. The 90 aa of ProPTH consist of the 84 aa of PTH plus a hexapeptide at the N-terminal end of the polypeptide (Habener, *et al*., 1976). ProPTH is transported within the smooth ER onto the Golgi complex where it is converted into PTH by a second proteolytic cleavage. PTH is then packed into secretory granules and secreted onto the extracellular fluid upon alterations in blood calcium concentration (Brewer Jr., *et al*., 1972).

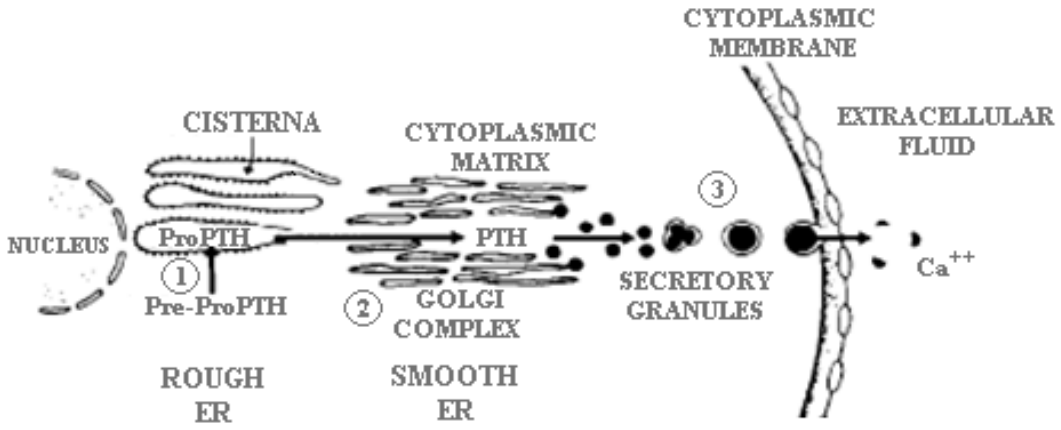

Figure 1.2 – Synthesis and secretion of the mammalian parathyroid hormone (PTH) in parathyroid glands. 1) Pre-ProPTH is synthesized in the rough endoplasm reticulum (ER) and is rapidly converted by proteolytic cleavage into ProPTH; 2) ProPTH is transported from the smooth ER to the Golgi Complex where through a second proteolytic cleavage it is converted into the mature PTH; 3) The hormone is transported to the extracellular fluid upon changes in blood calcium concentration (adapted from Habener, *et al*., 1976).

In humans, three mRNA transcripts are obtained by alternative splicing of the PTHrP pre-mRNA in a tissue-specific manner and under the control of different promoters (Clemens, *et al*., 2001). Three domains with specific biological properties and acting through distinct receptors can be found in all isoforms (Figure 1.3), N-terminal PTHrP region (1-36), that presents a 70% homology to PTH (1-34); a mid-region PTHrP (38-94) and a C-terminal PTHrP region (107-139) (Danks, *et al*., 2003). A unique region can be found in the 173 aa isoform (141-173) C-terminal region. The mid and C-terminal regions do not interact with the same PTH receptor and have no PTH-like activities, suggesting the existence of additional receptors (Clemens, *et al*., 2001).

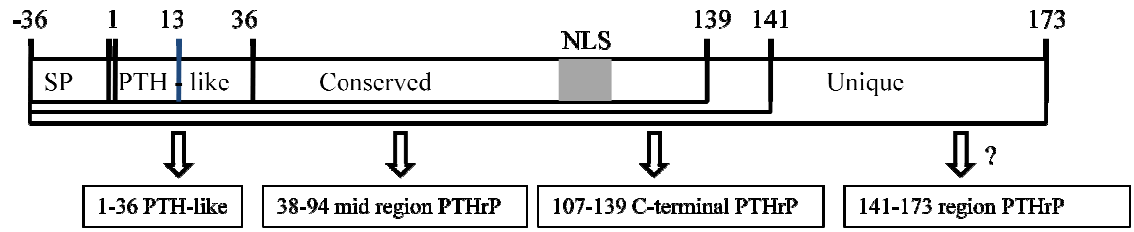

Figure 1.3 - Structure of the Parathyroid Hormone-related Peptide (PTHrP) isoforms in human. Alternative splicing gives rise to three different protein isoforms of 139, 141 and 173 amino acid long. The Signal Peptide (SP) is indicated (-36 to +1). Also, the Nuclear Localisation Signal (NLS) shaded grey is marked. The three bioactive domains are identified by arrows, the question mark indicates a possible forth domain. The first is the PTH-like domain with calciotropic function (adapted from Clemens *et al.* 2001)

The PTHrP gene contains also a Nuclear Localisation Signal (NLS) that presents the likelihood that PTHrP may also act through a nuclear pathway which involves the translocation of the nascent protein into the nucleus and not via the classical autocrine/paracrine pathway (Danks, *et al*., 2003; Gensure, *et al*., 2004). So far, in contrast to PTH, it was suggested that PTHrP presents multiple functional roles, such as, control of foetal development, transepithelial calcium transfer, lactation, smooth muscle relaxation and cell growth (Clemens, *et al*., 2001). The functions of PTHrP are related to its regions: the (1-36) PTHrP region has a PTH-like function and is involved in vasodilatation, differentiation and interacts with a similar type of receptor; the mid-region interacts with unknown receptors to maintain maternal-foetal gradients of calcium and magnesium in placenta and it is believed to have other functions; the (107-139) PTHrP region inhibits osteoclastic bone resorption and to date no function as yet been given to the (141-173) PTHrP unique region (reviewed in Clemens *et al.* 2001).

1.2 Receptors and signaling action

Peptide hormones (first messenger) are unable to pass through the cytoplasm membrane of their target cells and they exert their action by inducing the production of an intracellular signal (secondary messenger) on the cytoplasm surface of the plasma membrane (Fox, 1996; Campbell and Reece, 2005). The vertebrate PTH/PTHrP members interact with specific receptors members of the family 2 G-Protein Coupled Receptors (GPCRs).

1.2.1 G-Protein Coupled Receptors (GPCRs)

The GPCRs are the largest family of cell-surface molecules involved in signal transmission and their existence in the genomes of bacteria, yeast, plants, nematodes and other invertebrates suggests they are of early evolutionary origin (Kroeze, *et al*., 2003). The diversity of GPCRs is dictated both by the multiplicity of stimuli to which they respond, as well as by the variety of intracellular signaling pathways that they activate (Hermans, 2003; Kroeze, *et al*., 2003). Due to their diverse functions GPCRs were grouped into three major families that are recognized by different names: the family A (or family 1 or rhodopsin family), family B (or family 2 or secretin family) and family C (or family 3 or glutamate/GABA family) on the basis of sequence similarity (Bjarnadóttir, *et al*., 2006). The members of each family share over 25%

sequence identity for the transmembrane (TM) core region, and a distinctive set of highly conserved residues and motifs (Brown, 2000).

In general, GPCRs are characterised by a conserved molecular architecture consisting of seven TM helices that are connected by three extracellular (E1, E2, E3) and three intracellular (I1, I2, I3) loops; an amino-terminal extremity always located on the extracellular side which interact with the ligand and a carboxyl-terminus extending into the cytoplasm that mediates the intracellular signaling by activating an internal heterotrimeric G-protein (Figure 1.4) (Kroeze, *et al*., 2003). Depending on the type of G protein to which the receptor is coupled, several downstream signaling pathways can be activated (Figure 1.4), from which the adenyl cyclase (AC) and inositophospate (IP3) intracellular pathways are the most studied (Hermans, 2003).

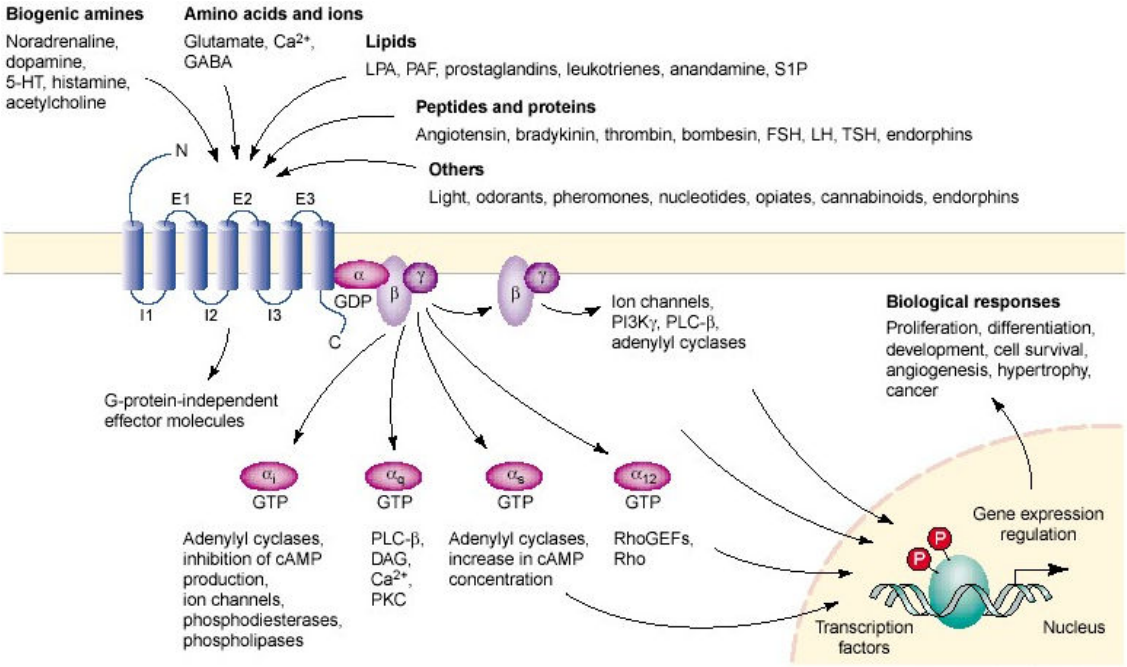

Figure 1.4 – GPCRs structure and multiple signaling pathways activated after ligand binding. The first step in signal transduction is the agonistic ligand binding followed by a change in the conformation of the receptor that may involve disruption of a strong ionic interaction between the third and sixth transmembrane helices which facilitates activation of the G-protein heterotrimer. Depending on the type of G protein and which receptor is coupled, a variety of downstream signaling pathways can be activated (adapted from Kroeze, *et al*., 2003).

1.2.2 Vertebrate PTH/PTHrP receptors

The PTH/PTHrP receptors are part of the family 2 GPCRs and all members of this family are characterised by the presence of large extracellular N-terminal domains with six conserved cysteine residues and N-glycolisation sites which are involved in the formation of the ligand-receptor pocket (Hoare and Usdin, 2001). In addition, the

extracellular loops and the extracellular end of the transmembrane segments are considered additional determinants of ligand selectivity (Runge, *et al*., 2003). In mammals, two PTH/PTHrP receptors (PTH1R and PTH2R) have been identified and whilst PTH1R binds both PTH and PTHrP the PTH2R favours PTH and the 39 amino acids of tuberoinfundibular peptide (TIP39) and to date no affinity of the PTH2R for the PTHrP has been demonstrated (Abbink and Flik, 2006; Danks, *et al*., 2003; Harmar, 2001). PTH1R and PTH2R have been mainly studied in mammals and recently homologues of the human receptors have been described in teleosts in which a third PTH receptor, named PTH3R was identified. PTH3R has a high degree of homology for the PTH1R and was proposed to have evolved through a gene duplication event (Gensure, *et al*., 2004). In chicken, two homologues of the vertebrate receptors have also been characterised and in *Xenopus* a similar number to the teleost PTH/PTHrP receptors were recently described (Gomes, 2007).

PTH regulates calcium metabolism by binding to PTH1R in bone and kidney, thereby activating the signaling pathway of adenylate cyclase and phospholipase C (Juppner, *et al*., 2001). The C-terminal portion of PTH (PTH (1–34) ligand) develops a highly ordered secondary structure upon contact with the N-terminal region of the receptor providing critical docking thereby inducing or selecting an active conformation that binds the preferential G-protein and thus begins the cascade of second messenger-mediated hormone-specific events within the targeted cells (Figure 1.5) (Potts, 2005; Hoare and Usdin, 2001).

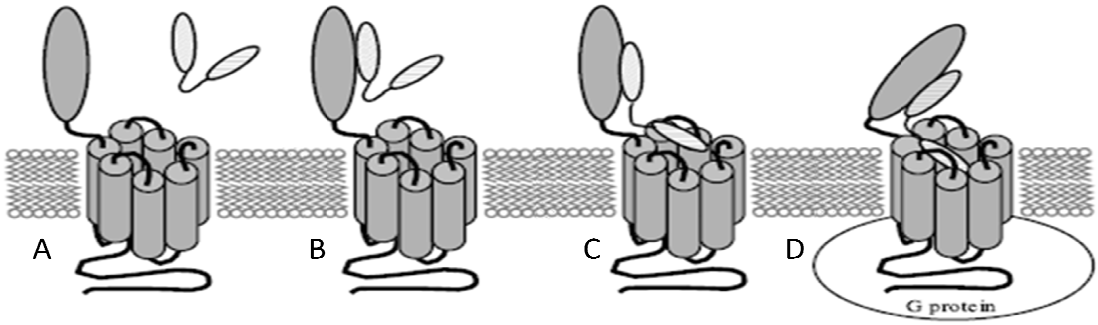

Figure 1.5 –Simplified model for the modulation of hormone binding and conformational modifications in GPCRs (A to D). A) Uncoupled receptor. B) The C-terminal portion of the ligand interacts with the *N*-domain of the receptor. C) Subsequently, the *N*-terminal portion of the ligand binds to the ligand-receptor pocket between the extracellular loops of the receptor. D) The interaction between the receptor and the G protein increases the affinity of the ligand with the extracellular loops and the receptor changes to a more closed conformation. D) In an equal manner, the interaction of the ligand with the extracellular loops domain increases the affinity of receptor for G protein, stimulating the G protein activation (adapted from Potts, 2005).

1.3 PTH/PTHrP functions

The utmost studied function of the PTH/PTHrP systems is the regulation of calcium blood concentration (Rolz, *et al*., 1999). Whilst PTH has a specific role in calcium metabolism, PTHrP is proposed to have a pleiotropic function and involved in multiple physiological activities (Ingleton and Danks, 1996). To date, the few reports on the description of the potential role of the PTH-L also suggest it may have an important role in calcium regulation (Canario, *et al*., 2006; Guerreiro, *et al*., 2007).

The PTH is known to have at least three distinct effects on calcium homeostasis in response to the low calcium concentration in blood (Hypocalcaemia). First, it increases the movement of calcium from bone to the extracellular fluid; Second, it stimulates the production of hydroxylating enzymes that convert vitamin D into the active form of vitamin D (hormone 1,25-DHCC) consequently stimulating the increase of calcium intestinal absorption. Finally, it increases renal tubular calcium reabsorption and as a result decreases calcium urinary excretion (Figure 1.6) (Vander, *et al*., 1985).

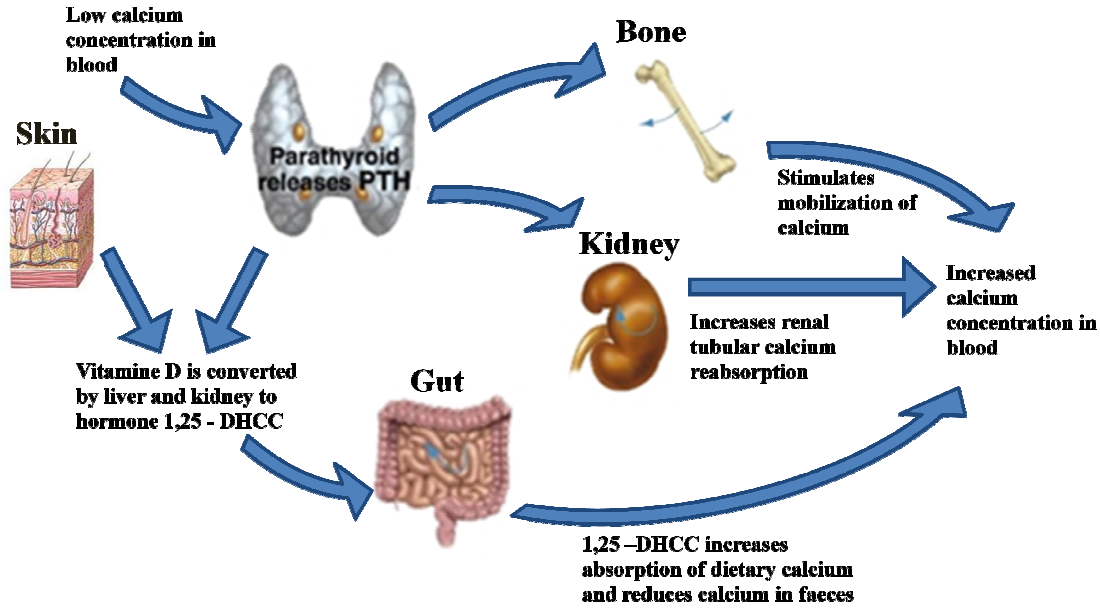

Figure 1.6 – Control and action of the parathyroid hormone in calcium balance. In response to low calcium concentration circulating PTH increases. PTH stimulates bone mobilization of calcium, renal tubular calcium reabsorption, and if hypocalcaemia is prolonged for several hours it induces the activation of vitamin D, which increases intestinal calcium absorption. These three actions induce an increase in blood calcium concentration (adapted from Mackenna and Callander (1997) and Winger, 1994).

The increase in calcium concentration induced by the PTH is counteracted by an antagonist hormone the calcitonin (CT) which is produced by the thyroid gland and completes the cycle of calcium homeostasis (Figure 1.7) (Campbell and Reece, 2005). In similarity with PTH, calcitonin acts in the same three different organs in response to the increase of calcium concentration: First, calcitonin acts in the bone osteoclats to prevent all stages of bone erosion avoiding the release of calcium into the blood. Second, it inhibits calcium reabsortion in the kidney which is consequently, excreted. Calcitonin has a negligible effect decreasing calcium concentration in the intestine by diminishing the calcium uptake (Brown, 2000).

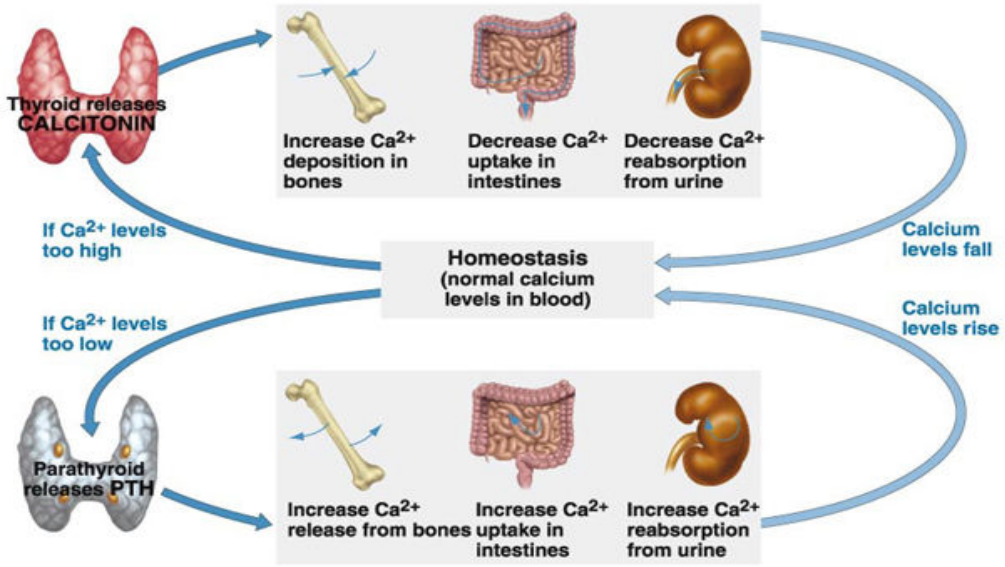

Figure 1.7 – Antagonistic actions of calcitonin and parathyroid hormone in calcium homeostasis. Parathyroid glands release PTH upon a decrease of calcium concentrations in the blood. PTH then acts on the bone to increase calcium release; acts indirectly on the intestines to increase calcium uptake and in the kidneys induces calcium reabsortion from the urine. Calcitonin maintains the calcium levels constant by decreasing the calcium concentration by a PTH antagonist action on the bone, intestines and kidneys (adapted from Campbell and Reece, 2005).

Although both hormones allow maintaining calcium levels carefully regulated, the steepness of the curve relating PTH and calcium concentration is the major contributor to its near constancy *in vivo* since small perturbations in calcium concentration elicit large changes in PTH release (Brown, 2000). Therefore, an increased or decreased secretion of this hormone is recognised as the cause of serious disorders that are classified into two groups: Hyperparathyroidism (excess of PTH) and Hypoparathyroidism (deficiency of PTH) (Gensure, *et al*., 2005).

A major disorder related with calcium balance is the Humoral Hypercalcemia of Malignancy (HHM). PTHrP overproduction was first reported in this disorder but PTHrP seems to have the role of local regulator of many physiological processes according to its localisation (Philbrick, *et al*., 1996). The main established physiological roles of PTHrP are the regulation of transepithelial calcium transport, regulation of smooth muscle tonus, tissue growth, cell differentiation and cell proliferation (reviewed by Philbrick, *et al*., 1996). A more detailed overview of PTHrP tissue-related functions was described by Clemens (2001) and summarized hereafter: PTHrP delays chondrocyte maturation, apoptosis and accelerates cartilage growth by promoting chondrocyte proliferation; regulates heart development; relaxes the uterus and vascular smooth muscle; interacts with calcium-binding proteins and calcium-sensing receptors to modulate trophoblastic growth and differentiation (Clemens, *et al*., 2001).

More functions have been reported to the calciotropic PTH-like region (1-36) PTHrP which is known to interact with PTH1R and stimulates bone resorption; in the skin the same ligand/receptor interaction promotes keratinocyte proliferation, delays keratinisation, apoptosis and terminal differentiation of epidermal keratinocytes; in kidney, PTHrP mimics all PTH-like effects on tubules and may have a role on glomerular development by interacting with PTH1R. Only two functions were assigned to the two other PTHrP regions: the (38-94) mid-region of PTHrP interacts with an unidentified receptor to maintain materno-foetal gradients of calcium and the region (107-139) PTHrP inhibits osteoclastic bone resorption (Clemens, *et al*., 2001).

1.4 PTH/PTHrP family members on skin

Merendino, *et al* (1986) were the first to explore the possibility that PTHrP could be expressed by normal epidermal cells since squamous cell carcinomas are the tumours most commonly associated with HHM. At least three distinct peptides have been shown to be produced in keratinocytes: (1-36) PTHrP region, the mid-region fragment beginning at amino acid 38 (Soifer, *et al*., 1992) and a heavily glycosylated mid-region PTHrP (Orloff, *et al*., 1993).

A number of factors have been shown to regulate the level of PTHrP mRNA expression and/or peptide secretion by keratinocytes in culture (e. g. 1,25-DHCC) (Philbrick, *et al*., 1996). Data from several studies indicate that PTHrP expression is inhibited by 1,25-

DHCC in normal cultured human keratinocytes (Kremer, *et al*., 1991). This is of importance because vitamin D (1,25-DHCC precursor) produced by keratinocytes is regulated by PTH and presumably by PTHrP (Philbrick, *et al*., 1996). While the normal physiological role of PTHrP in skin remains poorly characterised, the most studied effect of this peptide is on growth and/or differentiation of keratinocytes (Philbrick, et al., 1996).

Two tentative models to explain PTHrP actions in skin where proposed by Philbrick (1996):

- PTHrP is produced by differentiated keratinocytes in the outer layers of the epidermis and inhibits proliferation of basal and inner-layer keratinocytes.
- PTHrP produced by epidermal keratinocytes acts on dermal fibroblasts by coordinating epithelial-mesenchyme interactions during development.

The physiological roles for PTHrP in skin indicates that PTHrP acts most often as an autocrine or paracrine factor, for example, PTHrP produced by keratinocytes has effects on keratinocytes and on adjacent fibroblasts (Philbrick, et al., 1996). Most studies of the PTH/PTHrP family were performed with PTHrP due to its relation to skin cancer. PTH is known to require a synergistic effect of vitamin D to stimulate calcium influx (Stiffler, et al., 1998). Also, PTH induces cAMP production in skin fibroblast trough ligation with PTH1R receptor. In humans, the activation of the amino terminal region of PTH1R receptor was associated with cell proliferation and the absence of this receptor was associated with keratinocyte malignant transformation (Henderson, et al., 1992). PTH2R have been found to be expressed in skin although its physiological role is still unknown (Suarez, et al., 1995). To date, the receptor PTH3R and the peptide PTH-L were not identified in skin although functional studies using *Xenopus* and fish indicated that in this tissue PTH-L has a calciotropic function (Gomes, 2007; Guerreiro, et al., 2007).

1.5 Skin structure and function

The skin is the largest organ in the body (also known as the integumentary system) and forms a boundary between the body and the external environment providing protection against abrasion, ultraviolet light. Several functions are ascribed to skin and the most important are: production of vitamin D upon ultraviolet light exposure; prevention of

microorganism infection; prevention of dehydration; regulation of body temperature; and, excretion through skin and gland secretions. The skin is formed by main two layers: the dermis and the epidermis (Winger, 1994). The composition of human skin can be found in Figure 1.8.

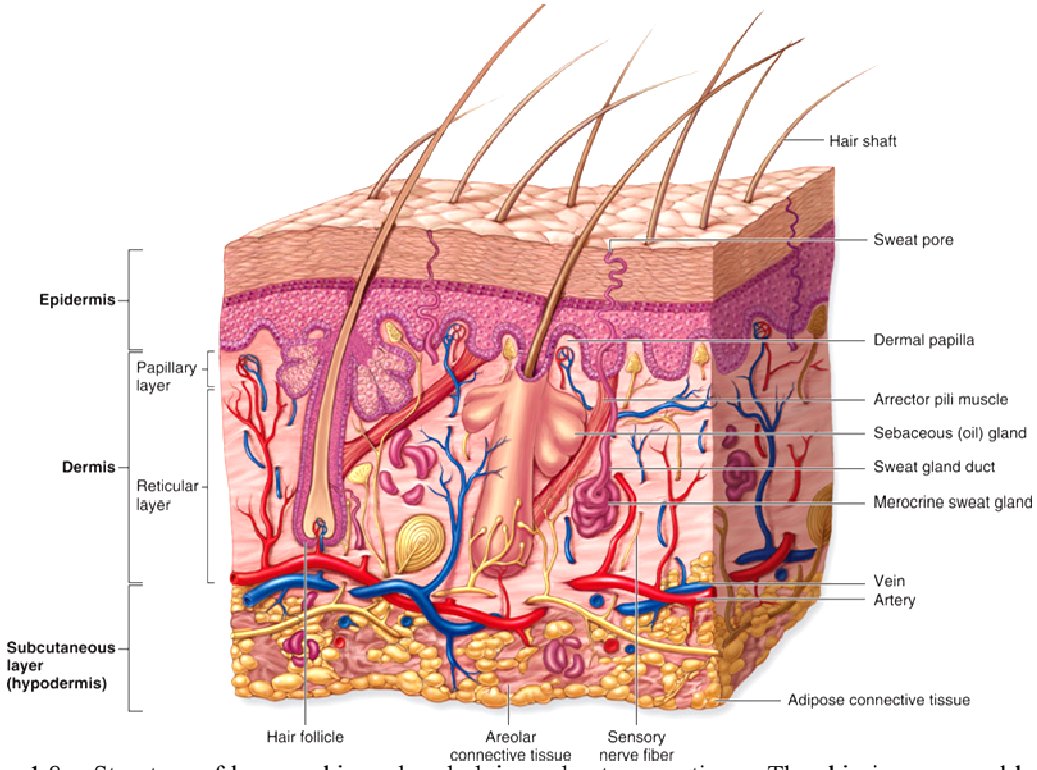

Figure 1.8 – Structure of human skin and underlying subcutaneous tissue. The skin is composed by the dermis and epidermis layers. Several small structures can be found in the skin: blood vessels, receptors and glands. The subcutaneous tissue is mainly composed by adipose tissue (adapted form Winger, 1994).

The dermis represents approximately 90 percent of skin thickness and is responsible for most of its structural strength. The dermis is mainly composed by collagen, fibroblasts, adipose cells, and macrophages. The main functions of the dermis are to regulate temperature and to supply the epidermis with nutrient-saturated blood (Tortora and Grabowski, 1996).

The epidermis is a complex stratified squamous epithelium formed by one basal layer that separates the epidermis from the dermis and several suprabasal layers/strata (corneum, lucidium, granulosum and spinosum) (Figure 1.9). The epidermis contains no blood vessels, and is nourished by diffusion from capillaries of the dermal papillary layer. Most epidermal cells are called keratinocytes and they produce keratin that protects epithelial cells from mechanical and nonmechanical stresses (Seeley, *et al.*, 2003). Other cells of the epidermis include melanocytes, which contribute to skin color

and provide protection against ultraviolet light; Langerhans' cells, which are part of the immune system; and Merkel cells, which are specialized epidermal cells associated with nerve endings responsible for detecting light touch and superficial pressure (Tortora and Grabowski, 1996).

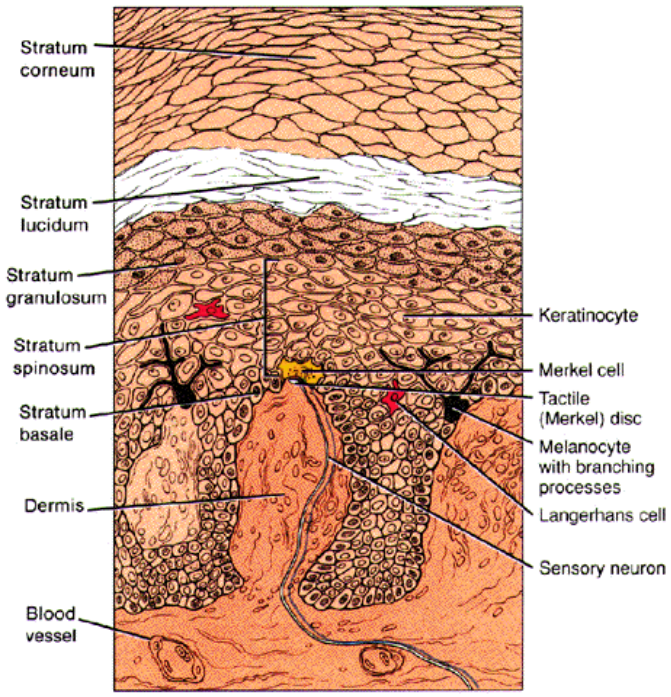

Figure 1.9 – Cell types and layers in the epidermis of thick skin. The epidermis is composed by five epidermal strata, namely: stratum corneum, stratum lucidum, stratum granulosum, stratum spinosum and stratum basale. The epidermis is mainly composed by keratinocytes but some merkel cells, melanocytes, lagerhans cells can also be found (adapted from Tortora and Grabowski (1996)).

Each epidermal layer contains keratinocytes at various stages of differentiation and proliferative potential. This division of epidermal cells is characteristic of the epidermis of all adult vertebrate species (Schreiber and Brown, 2003). Proper regulation of cell proliferation and differentiation is critical for the maintenance of the epidermis, and is centrally involved in its pathogenesis. Since, squamous cell carcinoma develops in keratinocytes that continue to divide as they produce keratin. Typically, the result is a nodular, keratinized tumor confined to the epidermis that can invade the dermis, metastasize, and cause death.

1.5.1 Stress (UV)-response system on skin

By being constantly subjected to the actions of solar and thermal energy, chemical and biological agents, the skin has developed unique properties to deal with these stressors. Thus, the skin is endowed with regional, local, and focal capabilities to recognize, discriminate, and to integrate specific signals within a highly heterogeneous

environment, and to integrate them into a stress-response neuroendocrine system (Slominski, *et al*., 2005). Development of squamous cell carcinomas may be promoted by UV-B exposure (Slominski, et al., 2005). Depending on wavelength and intensity, UV radiation can have broad-ranging effects in skin. It can provoke DNA damage, cell cycle arrest, and apoptosis as well as more specialized responses such as immunosuppression, activation of the p53 tumour suppressor protein, vitamin D synthesis, and sunburn/tanning. DNA repair and apoptosis are mechanisms that reduce the load of DNA damage and the number of damaged cells, respectively (van Oosten, *et al*., 2000). Severely UV-damaged epidermal keratinocytes undergo apoptosis (Goukassian, *et al*., 2004). Much of the UV response is due to the activation of mitogen-activated protein kinase family members through nuclear factor-B pathways leading to edema and erythema. UV response also regulates cell proliferation and apoptosis. Ultra-violet stimuli modulates hundreds of genes involved in diverse processes such as proliferation, apoptosis, inflammation, cell adhesion, and migration and the role of PTH/PTHrP systems in this process remains to be investigated (Madson, *et al*., 2006).

1.6 Experimental model (*Xenopus laevis*)

In this study, frog skin was used to evaluate the effect of UV-B light exposure on morphology and gene expression. Amphibians occupy an intermediate position in the adaptation to the terrestrial medium and frog skin constitutes a biological model suitable for studying physiological aspects of UV irradiation due to the lack of scales, hair or feathers (Leliñska, *et al*., 2005). Also, amphibians are tetrapods and their body plan is similar to that of mammals, providing important advantages over other model systems (Yergeau, *et al*., 2007). Researchers of the last century have used *Xenopus laevis* as a model system of choice to investigate numerous questions in developmental and cellular biology. Some limitations can be found in this species that the closely related *Xenopus tropicalis* does not have (Sartor, et al., 2006). A major advantage of the *Xenopus tropicalis* is that its genome is diploid while the *Xenopus laevis* genome is tetraploid. A drawback of *Xenopus tropicalis* is its small size that does not allow obtaining enough tissue for experiments. Therefore, in this work the two species were used: *Xenopus tropicalis* as a genomic model and *Xenopus laevis* as a physiologic model. Nowadays several databases can be found with molecular information from both species and the *Xenopus tropicalis* genome has been sequenced. Moreover, plenty of molecular databases can be found for *Xenopus laevi*s e *tropicalis*.

1.7 *Xenopus* PTH/PTHrP members

Human antibodies directed against PTH and PTHrP in amphibians revealed immunoreactivity in a variety of tissues of the frog *Rana temporaria* including the dorsal and ventral skin suggesting that PTHrP might have a role in tissue differentiation (Danks, et al., 1997). Recently, Gomes (2007) described the existence of PTH/PTHrP members and their receptors in amphibian using the genomic model of *Xenopus tropicalis*. In *Xenopus* two alternative splicing isoforms were identified, PTHrPA (131 aa) and PTHrPB (144 aa). Also, a homologue of the teleost PTH-L gene (168 aa) was described. The (1-34) PTH-like domain of all three members were demonstrated to have a potential calciotropic role in *Xenopus* skin. Although the biological action of PTH/PTHrP system in amphibian seem to be similar to other vertebrate, very little is known and only PTHrPB isoform was found to be expressed in skin (Gomes, 2007).

1.8 Objective

The aim of this project is to investigate the role of PTH/PTHrP family members in differentiation and proliferation on vertebrate skin model. The involvement of the PTH/PTHrP transcripts in UV-B response is to be evaluated in *Xenopus* skin using a combination of bioinformatics, molecular, and histological approaches. Genes with expression already evaluated, upon UV-B light exposure, are going to be used as a control/reference of the induced damage. The work will provide novel insight on the function/contribution of the PTH/PTHrP systems into the coetaneous response of frog skin to UV-B irradiation.

2. Material and methods

The material and methods used in this dissertation are described in this chapter. The experimental design adopted is illustrated in Figure 2.1. Sub-chapter 2.1.2 describes *Xenopus* species used in this work. The procedure used to expose skin explants to ultra-violet B (UVB) light is described in subchapter 2.2.1. The technical approaches used to evaluate the effect of UVB light exposure in *Xenopus* skin are organised in three major sections: 2.2.2) *in silico* analysis, 2.2.3) molecular biology approaches and 2.2.4) skin morphology characterisation. Reagents, buffers, media and primers used in each section are described in Annex I and II.

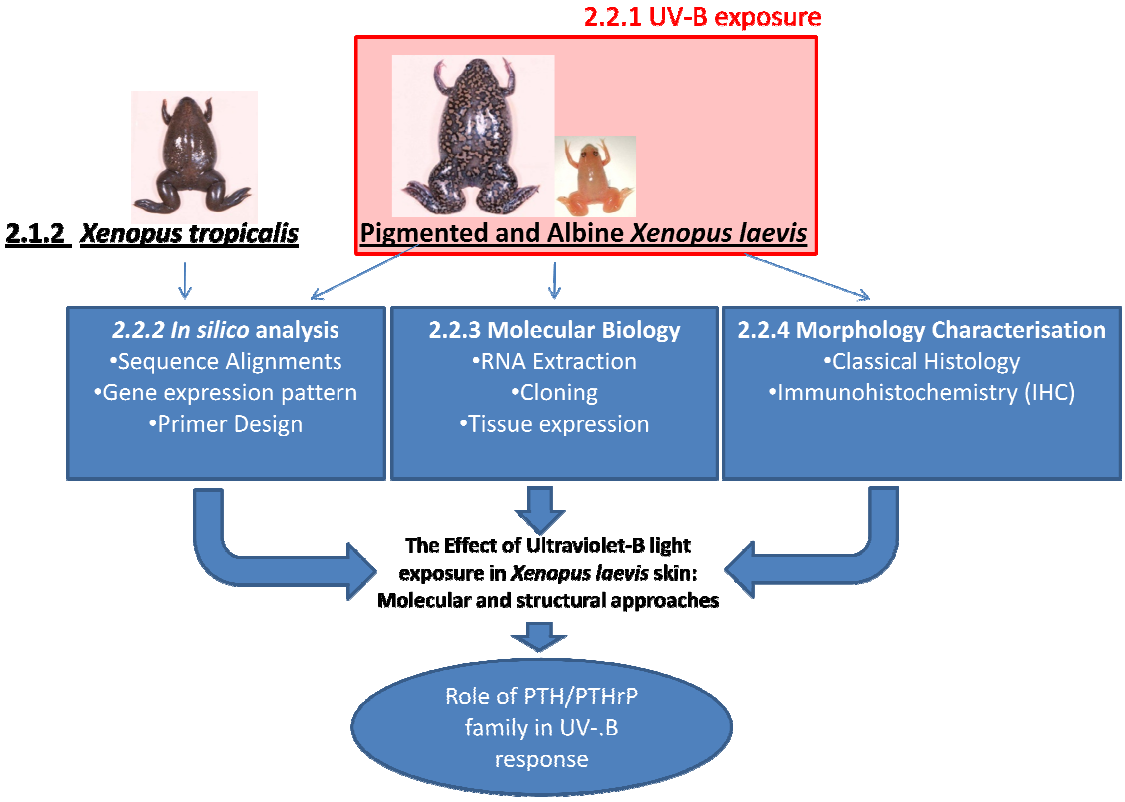

Figure 2.1 – Schematically overview of the material and techniques used during this dissertation. 2.1.2) The *Xenopus tropicalis* and the *Xenopus laevis* genome were used to perform in *silico* analysis (database search, sequence alignments, virtual gene expression and primer design). 2.2.1) *Xenopus laevis* pigmented and albino were exposed to UV-B radiation. 2.2.3) Tissues from Xenopus laevis were used in molecular biology assays (RNA extraction, RT-PCR, cloning and tissue expression). 2.2.4) Finally, the pigmented and albino *Xenopus laevis* dorsal skin were morphological characterised by histology and immunohistochemical methods. These three different approaches were used to evaluate the effect of UV-B light in *Xenopus laevis* skin and the role of PTH/PTHrP family members in this process.

2.1 Material

2.1.2 Biological model

In this study two *Xenopus* species (*Xenopus tropicalis* and *Xenopus laevis*) were used. *Xenopus tropicalis* was used as genomic model for *in silico* searches and two types of *Xenopus laevis* (adult pigmented and albino *Xenopus* froglets) were used to study gene expression in skin prior/after UV-B exposure. Normal adult pigmented *Xenopus laevis* were provided by Prof. José Belo group from Animal Cell Culture (FERN, University of Algarve, Portugal) and used to set up the experimental design and to retrieve preliminary results. The final experiment was carried out using albino *Xenopus laevis* froglets (Xenopus Express, France) due to the lack of pigmented adult *Xenopus* in the lab. Frogs and froglets were maintained in a tank with a closed water circuit at room temperature (RT) up to immobilization on ice for (5 min) and posterior sacrifice by double pitting. Several tissues were collected and immediately frozen in liquid nitrogen and stored at -80 ºC until further use. For UV-B exposure studies the extracted *Xenopus* dorsal skin was either stored at -80 ºC for molecular expression studies or immersed in 4% PFA for morphological characterisation and immunohistochemical (IHC) studies.

2.2 Methods

2.2.1 UV-B exposure – experimental design

In order to study the expression of PTH/PTHrP family members in skin damage/recovery, *Xenopus* dorsal skin was exposed to UV-B radiation and the following experiment was developed (Figure 2.2).

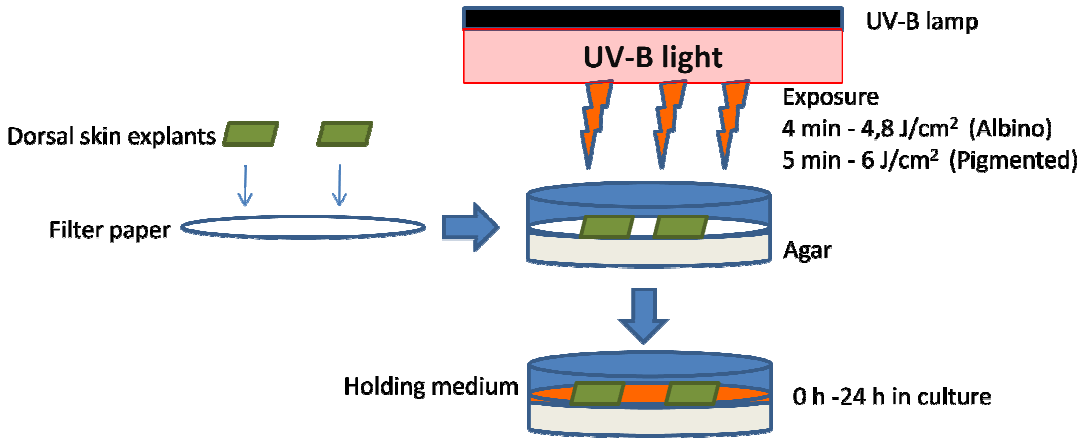

Figure 2.2 - Overview of the approach taken on *Xenopus laevis* skin UV-B exposure. The frog skin explants were laid above a filter paper and placed above a plate containing agar. The filter paper was moistened with holding medium and explants exposed to UV-B light by using an upturned transilluminator.

Before frog dissection, Petri dishes were prepared with 10g/L agar. The plates and holding media (MEM) were warmed at 26ºC. *Xenopus* skin extracted was placed on a filter paper and skin was transferred to a Petri dish with the epidermis uppermost. The filter paper was moistened with 1-2 drops of holding medium. Skin explants were then exposed for 4/5 min (4,8-6 J/ cm^2) to UV-B radiation provided by a Herolab UVT – 20 ME (6 tubes, 8 W, 312 nm) apparatus upturned covered with a box for user protection. Culture assays were developed at 26 ºC (Lavine, *et al*., 2005) and a controlled atmosphere of 5% CO_2 was provided inside plastic bags until sampling period.

PRELIMINARY EXPERIMENTS

In a first experiment, one adult pigmented *Xenopus laevis* was used for initial characterization of frog skin and to determine the minimal time where UV-B damage was observed. Skin samples were taken at 0, 2, 6, 12 and 24 h after UV-B exposure, cut in half and stored for RT-PCR and classical histology studies. A second experiment was performed to evaluate the potential effect of the culture time on skin structure. The control (without UV-B exposure) and UV-B exposed skin explants were maintained in culture and sampled at 0, 4 h after UV-B exposure. In both experiments frog skin was exposed to a UV-B radiation of 6 J/cm^2.

FINAL EXPERIMENTAL DESIGN

Preliminary experiments gave the indication that between 2 to 6 h after UV-B exposure morphological changes occur. Given that the objective was to observe initial gene expression changes due to UV-B response damage the final experiment was carried out at 4 h. The final experiment performed using 3 groups (group A, group B and group C with 4 individuals each) of albino *Xenopus laevi*s. A total of 12 individuals were chosen according to their size to minimize morphological variation between individuals. Group A was used as global control of the experiment (non-UV-B exposed and no media contact). Group B was used to evaluate skin morphological/molecular alterations due to culture time and was collected after 4 h in culture without UV-B exposure. In Group C frogs were UV-B exposed for 4 min (4,8 J/cm^2) and maintained in culture for 4 h. The decrease in exposure time in relation to the preliminary experiments was performed due to the assumption that albino *Xenopus* skin would be more sensitive than the normal pigmented skin due to the lack of chromatophores. Culture conditions and UV-B

exposure were developed according to the parameters described for the preliminary experiment. For the final experiment, dorsal skin explants were collected and after culture, cut in half and stored for subsequence molecular and morphological studies (Figure 2.3). Skin collection was made in the same related position in all individuals to minimise variation amongst groups.

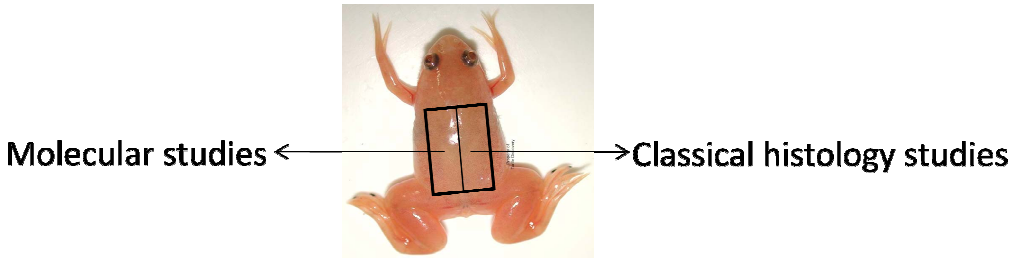

Figure 2.3 – Overview of the collection system used in the final experiment. Skin explants were taken of frog dorsal region and equivalent parts of the skin were used either for molecular studies or for Immunohistochemical studies.

2.2.2 *In silico* studies

Several molecular resources available for *Xenopus* genome were searched in order to identify the sequence of the incomplete PTH/PTHrP receptors 1 and 2 and to predict the expression of three biological markers chosen to evaluate the effect of UV-B exposure: keratin 8, collagen (type XVIII) and apoptotic gene p51/p63.

The N-terminal exon was missing from PTH receptor 1 and 2 and initial studies aimed to complete receptor structures. *Xenopus* gene sequences were obtained by searching the public available resources: Xenbase (http://www.xenbase.org/) and Ensembl genome browser (http://www.ensembl.org/). Potential gene fragments identified were isolated and translated using the program 6 Frame Translation from BCM Launcher – Bayor college of Medicine (http://searchlauncher.bcm.tmc.edu/) which allowed translating the protein sequence in its 6 reading frames. Sequence alignments were performed to compare predicted gene sequences with the homologues from other vertebrates to identify possible conserved patterns. Sequence alignments were performed using the mature amino acid sequences of the receptors using CLUSTAL X version 1.83 (Thompson, 1997).

ESTs are short (200–500 base pairs) DNA sequences that represent the gene expression profile in an organism under a given condition, acting has physical markers of the

expressed genes. ESTs are generated from the 3'- and 5'-ends of randomly selected cDNA clones from a determined species. Searches on *Xenopus* Expressed Sequence Tags (EST) databases for both *Xenopus tropicalis* and *laevis* were performed on NCBI EST resources to identify the first exon of receptor 1 and 2. Also, prediction of gene expression profile of some biological markers that could be used has a control of UV-B response was carried out. The genes were chosen upon their proven expression in human and *Xenopus skin*: keratin 8, collagen (type XVIII) and tumour protein p51/p63. The human genes were BLAST on NCBI database against *Xenopus* ESTs database to obtain gene homologues from where each gene specific primers were designed. The virtual expression profile was performed by BLAST search on *Xenopus laevis* EST databases and on Xenbase to evaluate from which tissue the EST had been isolated from.

2.2.3 Molecular Biology

Molecular biology techniques were used to characterise gene expression. In this study the gene expression of the *Xenopus* PTH/PTHrP receptors and their ligands, and some biological markers (keratin 8, collagen type XVIII) and the apoptotic gene (p51/p63) were investigated to characterise expression changes induced by UV exposure.

2.2.3.1 RNA extractions and purification

From each tissue, 50-100 mg was used for extraction yielding the RNA necessary for expression studies (1-5µg). Soft tissues were homogenized in 1 ml of TRI Reagent™ (Sigma-Aldrich™INC.) on a pestle homogeniser until a smooth homogenous suspension was obtained. Hard tissues (e.g. bone and cartilage) were macerated in a mortar using liquid nitrogen and then transferred to a tube containing 1 ml of TRI Reagent™ (Sigma-Aldrich™INC.). After an incubation period (5 min) at RT tubes were centrifuged at 13 400 *g* for 5 min at 4 ºC. The supernatants were transferred to a new tube and 200 µl of chloroform was added. The tubes were mixed vigorously for 15 sec and incubated 7 min at RT. The samples were then centrifuged at 13,400 *g* for 15 min at 4 ºC to separate the different phases. The upper aqueous phase (containing RNA) was transferred to a sterile tube where 500 µl of propanol-2 (isopropanol) was added. The tubes were incubated overnight (O/N) at 20 ºC. On the following day, precipitated RNA was obtained by centrifugation at 13 400 *g* for 30 min at 4 ºC. The pellet attained was washed twice with 200 µl of 75 % ethanol/DEPC. The pellet was air-dried

approximately 10 min at RT and resuspended in 50 µl DEPC-water. Extracted RNA quality was assessed in 1,5 % agarose gels and quantity determined in the Qubit® fluorometer (Invitrogen™). In skin samples where RNA quality was poor an additional purification step was used. A final concentration of 2 M lithium chloride was used on an O/N precipitation to eliminate potential protein contaminations that could interfere with cDNA synthesis.

2.2.3.2 DNA/RNA quantification

DNA/RNA concentrations were measured using Quant-iT™ RNA Assay Kit in the Qubit® fluorometer (Invitrogen™). For every trial, two tubes were set for the standards and one tube for each sample. In each standard tube 190 µl of working solution and 10 µl Standard from the kit was added. In each sample tube 199 µl of Working solution and 1 µl of sample was added. All tubes were shaken vigorously for a few seconds and incubated at RT for 2 min. After calibrating the Qubit™ fluorometer sample tubes were read.

2.2.3.3 cDNA synthesis

Extracted RNA was used to synthesize first-strand cDNA to be applied in the expression assays. In a sterile tube, 3 µg of total RNA was added in DEPC-water to a total volume of 29.6 µl. If there were not 3 µg of RNA in a sample (e.g. brain) the maximum volume was used (29.6 µl). Prior to cDNA synthesis RNA was denatured at 65 ºC for 10 min to melt secondary structure and cooled immediately on ice for 5 min. The final volume of 40 µl was achieved by adding to each reaction vial 8 µl M-MLV reverse transcriptase 5x buffer, 1 µl dNTPs (10mM), 1 µl random hexamers (1 µg/µl), 0.2 µl Recombinant RNasin® Ribonuclease Inhibitor (40 U/µl), 0.2 µl (200 U/µl) Reverse Transcriptase M-MLV (Promega® Corporation). After a short spin the samples were incubated for 2 h at 37 ºC. The reaction was inactivated by heating the tubes to 70 ºC for 15 min and cDNA samples were stored at -20 ºC until further use. The success of cDNA synthesis was verified by PCR with ribosomal 18s specific primers (Annex II).

2.2.3.4 Primer design

The primers used in PCR reactions with *Xenopus laevis* cDNAs were manually designed based upon the sequence of *Xenopus tropicalis* homologue genes. All primers were designed having in consideration the following parameters: G-C content higher

than 50%, approximate size 20 nucleotides and melting temperature around 55ºC (calculated with the assumption that any A/T nucleotide gives a 2ºC temperature increase contribution and any G/C base increases it by 4ºC). Primers were chemically synthesized and purchased from Sigma-Aldrich™ (Spain). All primers used have their characteristics described in Annex II.

2.2.3.5 Polymerase Chain Reaction (PCR)

Tissue expression was performed by RT-PCR using specific primers to evaluate the overall distribution of genes and potential change in expression due to UV-B exposure. PCR reactions were carried out with 2,5 µl 10x Reaction buffer, 0.75 µl 50 mM $MgCl_2$, 0.5 µl 50mM dNTP, 0,5 µl of forward and reverse primers (Annex II), 0.1 µl EuroTaq DNA polymerase (5U/µl) (EuroClone®), 1 µl cDNA and 19,15 µl of sterile water. Initially PCR reaction conditions were optimized using a temperature gradient and different concentrations of $MgCl_2$. The following PCR parameters were used: initial denaturation for 2 min at 9 4ºC, followed by 40 cycles of 1 min denaturising at 94 °C, 1 min annealing at Tm (^oC) (see Annex II), 1 min extension at 72 °C and a final extension of 5 min at 72 °C. The quality of produced cDNA was established by PCR using 18s primers (see Annex II) with the following parameters: cDNA was denatured for 3 min at 94ºC, followed by 25 cycles (94°C 35 sec, 57 ^oC for 1 min and 72°C for 45 sec), followed by a final extension of 5 min at 72 °C. All PCR products obtained were analysed on agarose electrophoresis gels (stained with ethidium bromide) under UV light and were sequenced to confirm identity.

2.2.3.6 Gel electrophoresis

Agarose gel electrophoresis was used to separate DNA/RNA fragments according to their molecular size. Agarose is a pored crossed polymer which allows migration of molecules according to their molecular weight. In this technique, samples containing DNA/RNA are loaded on gel and due to their negative charges they migrate towards the positive pole when exposed to an electrical charged field. Larger molecules have more difficulty to migrate so pore sizes can vary according to the percentage of agarose used. Therefore, depending on the size of the fragments to be analysed agarose gels of 1-1,4 % of agarose in TBE buffer (Sigma-Aldrich™, Spain) were used. Ethidium bromide (0,5 ng/ml) was added prior polymerisation. Ethidium bromide is a fluorescent dye that binds to DNA/RNA and is visible under ultraviolet light. To evaluate sample

migration and to give weight to the sample avoiding dilution of the sample in the running buffer, loading buffer was added to each sample before application onto the gel. As reference, 5 µl 1 kb molecular ladder was used to determine the size of the obtained products by comparison. All gel electrophoresis analysis ran with 100V and 220 A in horizontal gel trays containing 1x TBE buffer. DNA/RNA images were acquired using the AlphaEase®FC software (Alpha Innotech Corporation, USA).

2.2.3.7 DNA gel purification

DNA fragments were isolated from agarose gels using the GFX^{TM} PCR DNA and gel purification kit (Amersham Biosciences, Spain) according to the manufacture instructions when multiple PCR products were obtained and when primer-dimmers were formed. The correct DNA fragments were sliced-out from agarose gels and transferred to weighted *eppendorfs*. For each 10 mg of gel slice, 10 µl of capture buffer was added (max. 300 mg of gel) and mixed vigorously. The tube was incubated at 60 ^{o}C until the agarose was completely dissolved. Samples were loaded onto the GFX column to capture the DNA onto the glass fibre matrix. The tube containing the column was centrifuged at 13 400 *g* for 30 sec. The flow-through was discarded and 500 µl of wash buffer was added onto the column to remove salts and other contaminants. The tube was centrifuged as described above and the flow-through discarded again. Purified DNA was eluted from the column by adding 50 µl of water onto the column and after 1 min incubation the tube was centrifuged 1 min at 13 400 *g*.

2.2.3.8 DNA cloning

PCR products were cloned onto a vector prior sequencing. pGEM-T easy vector was used to clone PCR products. pGEM-T easy has resistance to ampicillin and allows positive bacteria selection on selective culture plates. pGEM-T easy also contains the operon Lac-Z, which is induced by IPTG, promoting the transcription of β-galactosidase that degrades the substrate X-Gal yielding in a blue colour substrate. Successful cloning of an insert into the vector interrupts the coding sequence of β-galactosidase and recombinant clones can be identified by colour screening on indicator plates containing IPTG and X-Gal. Clones that contain PCR products produce white colonies. All ligation reactions were performed for a total of 10 µl reaction mixture with 1,5 ng of vector pGEM-T easy (Promega, Spain) and approximately 3 times higher molar amount of insert DNA (ratio 3:1 – insert : vector). Also, 1 µl of T4 ligase (Promega, Spain) and 5

µl 2x T4 ligase buffer were added to the reaction mixture. The reaction was performed O/N at 4 ºC and used to transform bacteria competent cells.

2.2.3.9 Bacteria competent cells

Bacteria competent cells are able to incorporate exogenous genetic material and undergo transformation which is then maintained and replicated using cellular mechanisms. In this way several copies of a specific plasmid can be obtained. Calcium chloride method was used to prepare competent *E. coli* XL1-B. The competent bacteria cells were manually prepared by members of the MCE group. One colony isolated from a plate of LB medium (30 mg/ml tetracycline) was used to inoculate 5 ml of LB medium. Cells were incubated for 12-16 h at 30ºC and 250 rpm and 1 ml of this culture was used to inoculate 250 ml of SOB medium. The culture was then incubated with agitation at 18ºC until an optical density of 0.6 nm was reached. After, the bacteria suspension was incubated on ice to stop growth for 10 min, transferred to 50 ml *Falcon* tubes and centrifuged at 1 200 g for 10 min (4ºC). The supernatant was discarded and the pellet resuspended in 16 ml cold transformation buffer (TB), a solution rich in $CaCl_2$. The resuspended pellet was incubated on ice for 10 min and centrifuged as described above. DMSO (cryopreserving agent) was added until a final concentration of 7 % was reached. Bacteria were incubated on ice for 10 min, aliquoted in 100 µl tubes, frozen in liquid nitrogen and stored at -80 ºC until further use.

2.2.3.10 Cell transformation

Transformation allows a vector to be uptaken by a competent cell when a stimulus is applied. In this work, calcium chloride chemical method and heat-shock combined transformation were used to enable the *E.coli* XL1B competent cell membranes to allow the entrance of recombinant vectors. After thawing competent cells on ice 1 µl of plasmid DNA was added to the 100 µl of cells. The mixture was incubated for 35 min on ice mixing regularly. The heat shock transformation was performed by placing the tube in a 42 °C dry bath during 2 min and chilled afterwards for 5 min on ice. The cells were plated on LB agar plates containing 75 µg/ml amplicillin, 0,5 mM IPTG and 80 µg/ml x-gal. The plates were incubated O/N at 37º C. White colonies were isolated and used to set up liquid cultures. For the liquid cultures 5ml LB medium containing ampicillin was used. The tubes were maintained at 37º C O/N with agitation.

2.2.3.11 Plasmid DNA extractions (mini-prep)

Small amounts (3-5 µg DNA) of plasmid DNA were obtained by using single colonies to inoculate 5 ml LB medium containing ampicillin. Cultures were grown overnight at 37 ^{o}C with 250 rpm. From the culture 1.5 ml were centrifuged in an *eppendorf* at 12 000 *g* for 15 min (4 ^{o}C). The supernatant was removed and cells resuspended in 100 µl GTE to promote osmotic balance. GTE buffer contained 0,1 mg/ml RNase to destroy RNA. Lysis buffer (100 µl) was added to cell suspensions and incubated for 5 min at RT to induce cell lysis. Subsequently, 150 µl of 3M NaAc pH 5.5 was added to neutralise the mixture and the tubes were mixed by upturning 6 times. The tubes were centrifuged for 10 min at 13 400 *g* RT to *pellet* cell debris and chromosomal DNA. The clear supernatant was transferred to a new tube with 900 µl of 100% cold ethanol. The tubes were mixed, incubated 1 min at RT and centrifuged for 10 min at 13 400 *g* RT. DNA pellet was washed twice with 200 µl of 70% ethanol and centrifuged according to the previous parameters. The pellet was air dried and resuspended in 50 µl sterile water.

2.2.3.12 Restriction enzyme digestions

Restriction enzyme digestions were performed to evaluate the size of the cloned PCR fragments on pGEM-T easy vector. The vector MCS (*Multiple Cloning Site*) is flanked by the recognition site of EcoRI which can be used to release the insert. Reactions were set up for a final volume of 10 µl: 0.5 µl enzyme and 1 µl of 1x OPA buffer were used. The reaction was allowed to occur during 90 min at 37^{c}C and the results obtained visualised on agarose gels. If it was possible to see the vector and if the fragment band on gel had the expected size the clone was selected for further sequencing.

2.2.3.13 DNA sequencing

All DNA clones isolated were sequenced to confirm their identity. DNA sequencing reactions were carried out using T7 and/or SP6 primers and performed in CCMAR sequencing facilities and their quality analysed using chromatograms. Good sequencing reactions were chopped-off vector sequence and submitted to public databases to characterise their identity.

2.2.3.14 Statistical Analysis

In order to investigate the effect of UV-B radiation and culture time on the expression of five genes [Keratin 8, Collagen (type XVIII), p51/p63, PTH-L and PTHrP] a

statistical analysis was performed. The differences between three study groups were investigated using ANOVA with four skin explants used in each group. Data was analysed using SPSS® statistics version 17.0 (SPSS inc., Chicago, USA). When overall significance level was less than 0,05 a second stage of analysis included a post hoc test (Tukey) to evaluate which groups differed significantly from others.

2.2.4 Skin morphology characterisation

Classical histological studies were performed to characterise *Xenopus* skin and to evaluate the effect of UV exposure or of tissue culture time on skin morphology. Immunohistochemical (IHC) were tried to investigate protein distribution and expression based upon the binding of antibodies to specific epitopes.

2.2.4.6 Tissue fixation

Dissected frog skin was fixed in 4 % Paraformaldehyde (PFA) at 4ºC O/N. Fixed tissues were washed three times (15 min) with sterile PBS pH 7.4 and one time with sterile water before tissue processing. Tissues were transferred to 100 % methanol and stored at 4ºC until further use.

2.2.4.7 Processing and paraffin embedding

Paraffin-embedding hardens the tissue so that very thin sections, usually 4-5 μm, can be obtained. Tissue paraffin-embedding was done by enclosing the tissue in plastic cassettes and processed in a Leica TP1020 tissue processor (Meyer Instruments Inc., Houston, USA) according to the following program: 70% ethanol for 10 min, twice 95% ethanol for 30 min, twice 100% ethanol for 1 hour, ethanol : xylene (1:1) for 1 hour, xylene for 1 hour, xylene for 1,5 h, xylene : paraffin (1:1) for 2 h and paraffin for 2 h. Paraffin blocks containing the tissues in the correct orientation were prepared using 3 consoles: thermal, dispensing and cryo (Miles Scientific). It was considered a correct orientation when the transversal cuts of skin could be made.

2.2.4.8 Slides coating

Slides were made adhesive to tissues by coating with Poly-Lysine or aminopropyltriethoxysilane (APES) for a stronger adhesiveness to tissues. For the Poly-Lysine coating, slides were immersed in 0,5 % chloridric acid for 5 min and washed with running tap water for 5 min. Slides were then immersed in distilled water for 1 min

and subsequently immersed in 0,01 % Poly-Lysine for 5 min. Slides were left to dry in an oven at 37 ºC O/N or at 60 ºC for 1 h. When coating with APES slides were cleaned in 1 % Acid/Alcohol, rinsed in running tap water, immersed in distilled water and allowed to dry. Slides were then immersed 10 min in acetone and 5 min in 2% (v/v) APES. Slides were finally rinsed briefly twice in distilled water and allowed to dry.

2.2.4.4 Sectioning of skin samples

Paraffin blocks containing skin were cut in a microtome with thicknesses of 5 µm. From Tissue sections were mounted on a microscope slide (coated with Poly-Lysine or APES) and dried overnight. These slides were used after paraffin removal either for staining with appropriate dyes or for IHC.

2.2.4.5 Haematoxylin-Eosin (H&E) staining

Haematoxylin-Eosin (H&E) staining method involves the application of haematoxylin (basic dye), which colours basophilic structures blue/purple, and alcohol-based acidic eosin Y, which colours eosinophilic structures bright pink. Basophilic structures are usually the ones containing nucleic acids, such as ribosomes, cell nucleus, and cytoplasmatic RNA rich regions. Eosinophilic structures are generally composed of proteins and dye generally the cytoplasm. Prior staining, tissue sections were hydrated by washing, twice for 15 min with xylene, 5 min through each graded ethanol: 100%, 95%, 70% and 5 min through distilled water. Slides were immersed in haematoxylin for 30 sec, washed with tap water with a few drops of 4 M ammonia and washed again with tap water. Slides were then immersed in Eosin Y for 30 seconds, washed with distilled water with a few drops of acetic acid and rinsed with distilled water. Dehydration was made through graded ethanol: 70%, 95% and 100% for 5 min each. Slides were then immersed twice for 15 min in K clear and mount using DPX resin.

2.2.4.6 Masson Trichrome staining

Masson's trichrome, a three-colour staining protocol was used to distinguish cells from surrounding connective tissue. This staining colours the nuclei black, cytoplasm and muscle colour red and collagen is coloured green. Prior staining, tissue sections were hydrated by washing twice for 10 min with xylene and 5 min through each graded ethanol: 100%, 95%, 70% and distilled water for 5 min. Slides were immersed in Mayer’s haematoxylin for 10 min, washed with running tap water for 5 min and washed

again with distilled water. Slides were then immersed in Xylidine Ponceau for 2 min and washed with distilled water for 5 min. Slides were for last immersed in Light Green for 90 sec and dehydrated rapidly through graded ethanol: 70%, 95% and 100%. Slides were immersed twice for 15 min in K clear and mount in DPX resin.

2.2.4.7 Alcian Blue staining

Alcian Blue staining was used to differentiate between neutral and acetic mucosubstrates, which colour respectively magenta and blue. Prior staining tissue sections were hydrated by washing twice for 10 min with xylene, 5 min through each graded ethanol: 100%, 95%, 70% and 5 min through distilled water. Slides were immersed in Alcian Blue for 30 min, washed with running tap water for 5 min and rinsed in distilled water. Slides were then immersed in 0,5 % periodic acid for 5 min and washed with distilled water for 5 min. Slides were immersed in Schiff's reagent for 30 min and washed with distilled water for 5 min. Slides were then immersed in Gill's Haematoxylin for 3 min and washed in running tap water for 5 min. Slides were rinsed in distilled water and dehydration was made through graded ethanol: 70%, 95% and 100% for 5 min each. Slides were immersed twice for 15 min in K clear and coverslipped using DPX resin.

3. Results and Discussion

The results and discussion of this thesis are organized in three major sections: 3.1) *Xenopus* PTH receptors, 3.2) Structural characterization of *Xenopus* skin and 3.3) Molecular characterization of *Xenopus* skin UV response.

3.1. *Xenopus* PTH receptors

In *Xenopus*, three potential PTH/PTHrP receptor homologues of the teleost (PTH1R, PTH2R and PTH3R) and mammalian genes (PTH1R and PTH2R) were previously identified using *in silico* comparative approaches (Gomes, 2007). In this previous study, *Xenopus* receptors were found to share identical gene structure with the vertebrate homologues. *Xen*PTH3R was fully characterised and the sequence of the remaining receptors (*Xen*PTH1R and *Xen*PTH2R) was incomplete, missing the first exon region. In Annex III, PTH/PTHrP receptors gene structure of human, teleost and *Xenopus* can be found. Exon 1 encodes for the receptor's signal peptide (SP) region which is responsible for appropriate anchoring of the receptor to the cell membrane (Joun, *et al*., 1997) and the completion of the receptor sequences is essential to ensure correct receptor folding and integration in the membrane.

The initial aim of the present project was to isolate the lacking first exons of *Xen*PTH1R and *Xen*PTH2R in order to amplify the full clones. The complete receptors are going to be used in the future in cell expression assays to characterise their functional profile in the presence of *Xenopus*, teleost or human PTH/PTHrP family members. I*n silico* comparative approaches and data mining searches were performed. *Xenopus* available molecular data (genome and EST) found in Ensembl, NCBI and Xenbase was interrogated with the exon 1 region of vertebrate homologue receptors to identify similar regions. Also, analysis using the receptor 5' genomic regions prior to exon 2 using prediction programmes (e. g. ExonScan Web Server (http://genes.mit.edu/exonscan/)) was performed.

In *Xenopus tropicalis* genome assembly, *Xen*PTH1R is located in scaffold 479 and *Xen*PTH2R maps to scaffold 264. Sequence comparisons of the vertebrate PTH1R first exon regions previously isolated share very little sequence similarity and despite the conservation in length of the encoded peptide (25 amino acids long) only few amino acids are maintained (Table 3.1). These results are in agreement with the features of family 2 GPCRs where poor sequence conservation exists for the N-terminal and C-

terminal regions when compared with the conserved core of the seven TM sequence block (Kamesh, *et al*., 2008).

Table 3.1 - Multiple sequence alignment of the 25 amino acid of vertebrate PTH1R encoded in exon 1. Conserved amino acids across all species analysed are shaded. Similarity percentages of several vertebrates with human sequence were calculated using GeneDoc version 2.6.003 (www.psc.edu/biomed/genedoc).

Organism	Sequence	Similarity (%)
Human	MGT ARI APG LA- LLL CCP VLS SAY AL	100
Rat	MGT ARI APS LA- LLL CCP VLS SAY AL	96
Chicken	MGS YLV YHS LG- LIL CCS VLS SVY AL	68
Takifugu	MGA TLI VRT LG- FLF CCT LLF STW CL	56
Zebra fish	MGS SLR RCC LCC LLL CCA -LS FVY GL	48

In vertebrate, the conserved amino acids of PTH1R first exon are Met[1], Gly[2], Leu[10], Cys[15], Cys[16], Leu[19] and Leu[25]. Characterisation of receptor's intron-exon boundary phases showed an established phase 0 (zero) maintained across all studied vertebrates (Gomes, 2007). The preceding conserved characteristics (length, sequence conservation and intro-exon phase) were used to search for homologue regions in *Xenopus* genome. Approximately 69 kb prior to exon 2 region was extracted and submitted to exon prediction programs. The five probable exons localisations with a phase 0 intron-exon boundary phases were identified upon length however in depth analysis revealed that they did not fulfil the sequence conservation requirements. Therefore, the first exon of PTH1R remains to be isolated. One of the reasons that contributed for this failure is the poor sequence quality data within the analysed region.

A similar strategy was used to identify a potential localisation of *Xen*PTH2R exon 1. Multiple sequence alignment of the first exon of vertebrate PTH2R revealed that they share little sequence similarity and only two conserved amino acid positions were identified, Leu[20] and Glu[25]. Moreover, in common with PTH1R the putative *Xen*PTH2R exon 1 has an intron-exon boundary phase 0 (zero) (Gomes, 2007). Sequence comparisons also revealed that its size differed between the compared organisms and a shorter exon 1 sequence was identified for chicken and mammal genes (25 amino acids long) (Gomes, 2007). The extracted 30 kb genomic region prior to *Xen*PTH2R exon 2 was analysed manually and using exon prediction programmes. This lead to the identification of a potential exon 1 at 29 kb prior to the second exon which fulfilled the predetermined sequence criteria (Figure 3.1).

```
ATG AAT CCT GAA AAA TTA AGT GAA GAG GTT TGG CAA TCA CAG CGC TCA CCT
 M   N   P   E   K   L   S   E   E   V   W   Q   S   Q   R   S   P
CAT TTA ATA CCC TGG GAT GAA TCC CAT CCG GCC CTG GAC CTT TGT TTA CCT
 H   L   I   P   W   D   E   S   H   P   A   L   D   L   C   L   P
TTA TAT GTT CAA
 L   Y   V   Q
```

Figure 3.1 – Predicted sequence (nucleotide and amino acid) of the first *Xen*PTH2R exon. Amino acids that are found to be conserved are shaded.

The identified sequence is 38 amino acids long and contains the two conserved amino acids positions Leu^{20} and Glu^{25}. Specific primers for this region were designed (Annex II) and a PCR product was obtained although after cloning and sequencing it was not conclusive. Therefore, further work will be needed to determine *Xen*PTH2R first exon identity.

Besides genomic analysis, searches on available EST were also performed to complete the *Xenopus* PTH1R and PTH2R. *Xenopus* EST databases (NCBI BLAST (txid 8353, txid 262014) and Xenbase (*Xenopus tropicalis* ESTs) were used in order to identify potential novel ESTs that could contain signal peptide sequence. Using partial sequences of *Xen*PTH1R and *Xen*PTH2R ESTs were retrieved (Table 3.2).

Table 3.2 – Accession numbers of the Xenopus PTHR receptor ESTs identified in the NCBI and Xenbase *Xenopus* databases.

Receptor	EST
PTH1R	Cx929442.1
PTH2R	None
PTH3R	CF780983.1
	DN014042.1
	DN000185.1
	DR717982.1
	NM_001011042.1

A single EST clone was identified for *Xen*PTH1R (Cx929442.1) and for *Xen*PTH2R no homologues are annotated in the databases. Comparison of the *Xen*PTH1R EST revealed homology for the middle receptor region and did not contain the signal peptide. Therefore, *Xen*PTH1R complete sequence remains to be identified. The majority of identified ESTs correspond to the already fully sequenced PTH3R (Gomes, 2007) for which a total of five ESTs are annotated: CF780983.1, DN014042.1, DN000185.1, DR717982.1 and NM_001011042.1. The results obtained confirmed the previous studies carried out by Gomes (2007) and no other ESTs are so far annotated.

The complete sequence of *Xen*PTH1R remains to be determined despite the extensive *in silico* comparisons and database searches carried out. The failure to identify the full

*Xen*PTH1R was due to the poor sequence quality available for this region and to the lack of ESTs. The potential exon 1 for *Xen*PTH2R identified needs further confirmation. In future, alternative methods, such as RACE 5' regions can be used to determine the missing receptor sequences in order to proceed with the mammalian cell assays.

3.2 Structural characterisation of the *Xenopus laevis* skin

In order to characterise and identify potential modifications induced by UV-B exposure pigmented *Xenopus laevis* dorsal skin three different staining methods were applied to *Xenopus* skin histological sections: Haematoxylin-Eosin Y (H&E), Masson's trichrome and Alcian Blue. H&E staining was used to obtain a general idea of the quality of the histological preparations and of *Xenopus* skin structural organisation. Masson's trichrome staining was used to distinguish between skin layers: epidermis and dermis. Finally, a more specific staining (Alcian Blue) was used to identify and distinguish skin glands content.

Haematoxylin-Eosin Y staining

H&E staining allows the identification of a range of structures: nucleic acids found in the nucleus were stained purple, the cytoplasm and other cell structures with protein content stained pink (Figure 3.2).

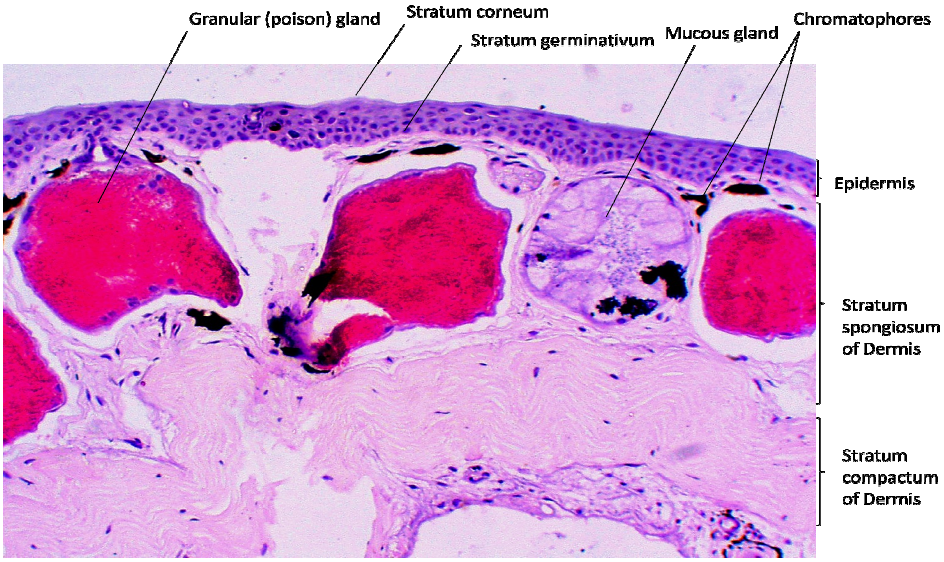

Figure 3.2 – General overview of a section through an adult pigmented *Xenopus laevis* skin. Two main layers can be distinguished: the epidermis and the dermis. The epidermis is composed of several stratified cellular layers. The dermis is further divided in two layers: the stratum compactum composed mainly by collagen and the stratum spongiosum of dermis that contains mucous glands and granular (poison) glands. Chromatophores are also located in the stratum spongiosum of the dermis.

Frog skin is composed of the two well defined layers (Kardong, 1998): epidermis and dermis. In the epidermis multiple layers of squamous cells with a well stained nucleus in purple were observed (Figure 3.2). A well organised layer of cuboidal basal epithelial cells marks the limit between the epidermis and the dermis. The dermis can be further divided into two layers the stratum spongiosum and the stratum compactum. In the dermis immediately below the epidermis two types of glands previously described in frog skin were observed: granular (poison) glands and mucous glands which are known to increase in size as the animal grows (Engelmann, 1872).

Granular glands

Intensely pink staining granular glands are clearly visible (Figure 3.2). The granular glands are composed of ellipsoid-shaped secretory granules (Lacombea, *et al*., 2000). The granular glands connect to the external environment through epidermal ducts (Dockray, *et al*., 1975), as seen in the first granular gland shown in Figure 3.2. Granular skin secretions of amphibians have been studied due to their evolutionary relation with mammalian sweat glands (Davis, *et al*., 1979) and they were reported to secrete large quantities of various peptides upon stimulation (Flucher, *et al*., 1986). The excretion of the granular content seems to be related with defence mechanisms (Davis, *et al*., 1979).

Mucous glands

Mucous glands are slightly smaller than granular glands (Dockray, *et al*., 1975). This difference in size could not be demonstrated in this work because the section through was not in the centre of each gland. Mucous glands show cubical-cylindrical cells and lumen material appear to be fibrillar (Figure 3.2). This sort of structure was also observed in other frog species, namely the *Rana ridibunda* (Sengezer-Inceli, *et al*., 2004). In similarity with this species, *Xenopus laevis* also presents small mucous glands that appear not to contain any secretory material in their lumen and are mainly composed of cubical cells (Figure 3.2). The function of mucous glands seems to be facilitating skin thermoregulation (Davis, *et al*., 1979). It was concluded by Lillywhite (1971) that mucous glands of *Rana catesbeiana* discharge lumenal fluid onto the surface of the epidermis synchronously and periodically as a response to sympathetic nervous stimulation (Lillywhite, 1971). It was not observed any mucous gland where the content had been discharged.

Chromatophores

Chromatophores were observed in the stratum spongiosum of dermis (Figure 3.2). Chromatophores are pigment-containing cells that generate the skin colour. Amphibian skin contains melanophores, a black/brown chromatophore-type which are the equivalent of the human pigment cell type the melanocytes (Fingerman, 1965). In general, skin darkness correlates closely with the number, size and dispersal of melanosomes (April and Barsh, 2007).

Masson's trichrome staining

Masson's trichrome staining is a more complex mixture of pigments than the ones used in H&E staining that allows differentiating cells from connective tissue. This staining method results in black staining nuclei, red staining cytoplasm and turquoise staining collagen. In Figure 3.3a) and 3.3b) it was possible to observe in the dermis a large layer of turquoise connective tissue rich in collagen. This is a characteristic organisation of vertebrate skin and has been previously described in several amphibians, including the species *Bufo ictericus* and *Rana catesbeiana* (Azevedo, *et al*., 2006) The dermis is subdivided in stratum spongiosum comprised of loose connective tissue and in stratum compactum with collagenous fibres compactly structured (Kardong, 1998). Collagen fibres surround skin glands and also form a continuous layer at the interface between the dermis and epidermis in a clear separation of the two layers (Figure 3.3a, b and c). With Masson's trichrome, mucous glands are not stained and granular glands present high protein content stained in red. Granular and mucous glands, located in the dermis, secrete to the epidermis surface through short ducts made of epidermal cells (Figure 3.3a and c) (Dockray, *et al*., 1975). Although, formation of granular glands takes place during metamorphosis a steady *de novo* formation of new glands occurs in adult animals (Flucher, *et al*., 1986). This stage of premature granular glands could also be observed (Figure 3.3b) called vacuolated stage (Dockray, *et al*., 1975). At this stage it is not possible to identify any secretory granules because cell membranes within the gland have already disintegrated no mature granules have yet been formed (Flucher, *et al*., 1986). The high protein content can be already predicted by highly red staining of the gland at this stage (Figure 3.3b).

Alcian Blue staining

Alcian Blue staining was used to differentiate neutral and acid mucosubstrates, which colour respectively magenta and blue. With this staining it was possible to determine

that *Xenopus* mucous is acid due to highly blue staining observed in mucous glands (Figure 3.3d). The acid content of mucous glands was also documented in other frog species, like *Rana pipiens* where mucous was assumed to be a mixture of carboxylic and sulphate acids (Dapson, 1969).

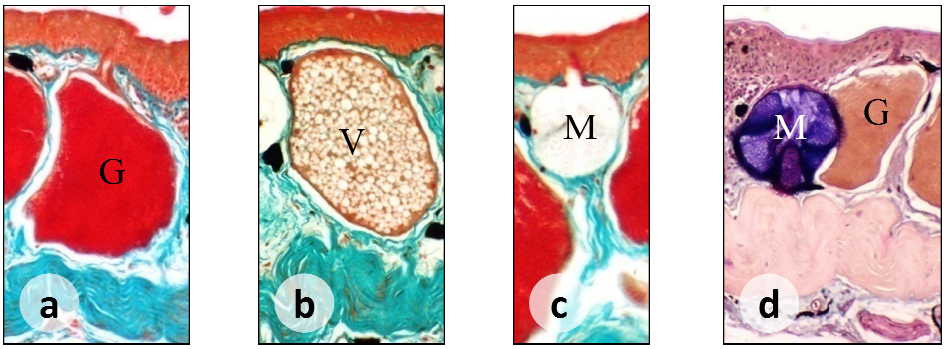

Figure 3.3 –Section through a normal *Xenopus laevis* skin stained with Masson's trichrome (a, b and c) and Alcian Blue (d) showing mature granular glands (G), granular gland vacuolated stage (V) and mucous glands (M). With Masson's trichrome collagen fibres stained green and the epidermis stained red (a, b and c) and the high proteic content of granular glands was stained in red (a, b and d). Mucous glands present no staining (c) with Masson's trichrome or acidic content in blue with Alcian Blue (d). [Amplification 10x (a, b and d), 20x (c)]

Structural characterisation of UV-B exposed skin

Histological sections of UV-B exposed *Xenopus* skin were also subjected to the same staining procedures described previously to identify morphological alterations. For this, skin without UV-B exposure was used as a control of observed alterations and UV-B exposed skin was kept for varying lengths if time in culture medium to establish the time where morphological changes induced by UV-B exposure start. A summary of the major alterations observed are indicated in Table 3.3 and shown on Figure 3.4.

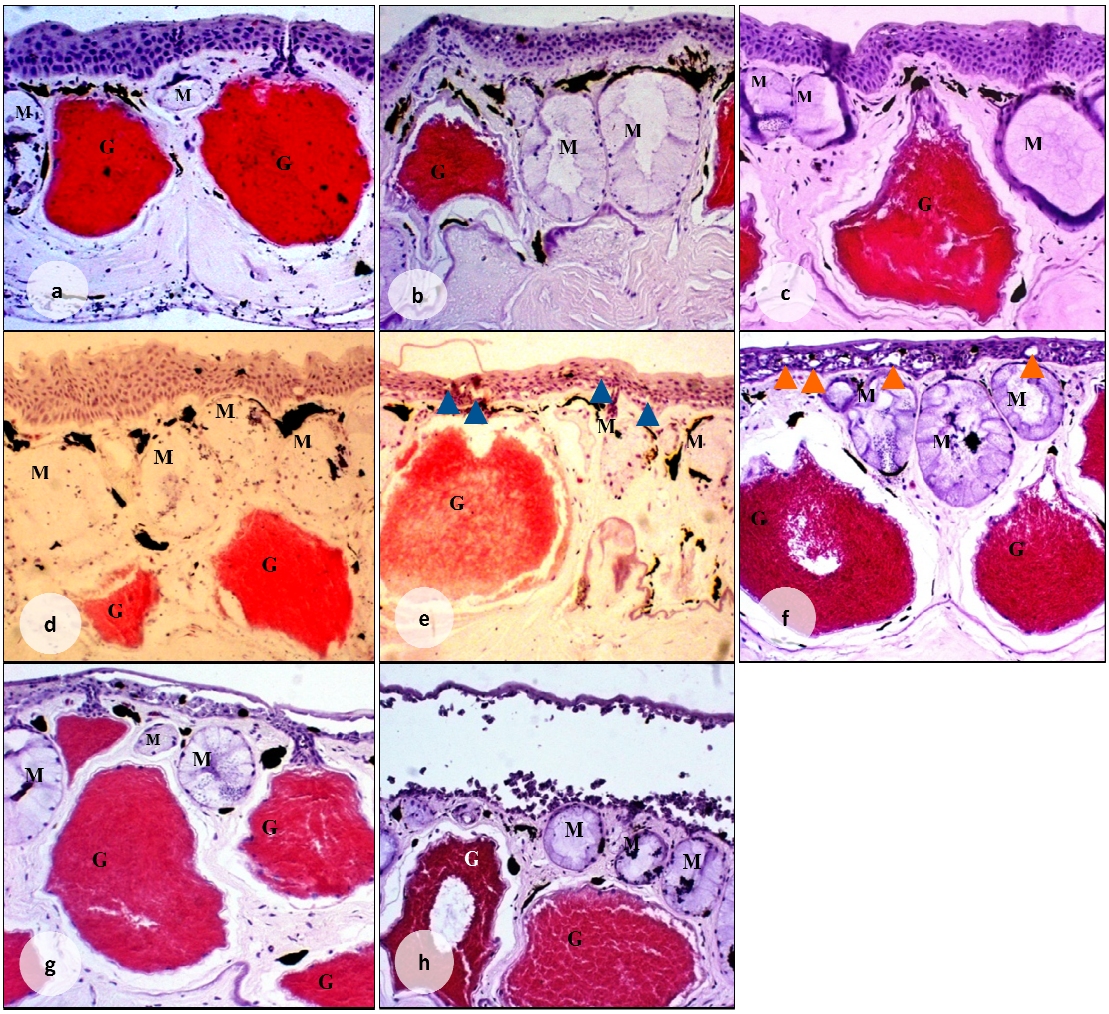

Figure 3.4 – H&E staining of several section through adult pigmented *Xenopus laevis* skin. a) control skin non cultured/UV treated d) control skin after 4 h in culture; UV exposed skin and contact with culture media after (b) 0 h (c) 2 h, e) 4 h, f) 6 h, g) 12 h and h) 24 h). Granular (G) and Mucous (M) glands are indicated [Amplification 10x]. (Blue (f) and orange (e) arrow-heads represent places where apoptosis occurred)

In normal frog skin (Figure 3.4.a), as described above, granular and mucous glands located in the stratum spongiosum of dermis layer and a stratified epidermis with a small duct can be observed.

Table 3.3- Outline of the variety of effects induced by UV-B exposure at different times when compared to normal skin*. These preliminary observations were based in only one individual. (*without UV-B exposure)

<table>
<tr><th>Time</th><th>Granular glands</th><th>Mucous glands</th><th>Epidermis</th><th>Dermis</th><th>Chromatophores</th></tr>
<tr><td>control*
(Figure 3.4a)</td><td>Granular glands were full of highly red stained granules (fuse shape).</td><td>Cluster of cells can be seen inside the gland.</td><td>Squamous epithelial cells arranged in tight layers upon the basal layer. Short ducts from glands into the surface of epidermis can be seen</td><td>Granular glands and mucous glands were surrounded by connective tissue in the stratum spongiosum. Some fibroblasts can be seen in the connective tissue in the lower regions of dermis.</td><td>Scattered throughout the dermis and surrounding the granular and mucous glands</td></tr>
<tr><td>0 h
(Figure 3.4b)</td><td>No relevant changes</td><td rowspan="4">No relevant changes</td><td>No relevant changes</td><td rowspan="2">No relevant changes</td><td>No relevant changes</td></tr>
<tr><td>2 h
(Figure 3.4c)</td><td rowspan="3">Content not as compact</td><td>Upper layer of epidermis seems to be separating</td><td rowspan="4">No relevant changes</td></tr>
<tr><td>4 h control*
(Figure 3.4d)</td><td>No relevant changes</td><td rowspan="3">Mucous gland migration to regions closer to the epidermis and consequently granular glands were pushed to lower region of stratum spongiosum</td></tr>
<tr><td>4 h
(Figure 3.4e)</td><td>Separation of basal layer of epidermis and some cells from the interior layer disappeared</td></tr>
<tr><td>6 h
(Figure 3.4f)</td><td rowspan="3">Reduced granular content</td><td rowspan="3">Mucous glands appear smaller</td><td>Degradation of the interior layers of epidermis</td></tr>
<tr><td>12 h
(Figure 3.4g)</td><td>Stratum corneum of epidermis and basal layer were apart</td></tr>
<tr><td>24 h
(Figure 3.4h)</td><td>Stratum corneum of epidermis and basal layer were apart</td></tr>
</table>

UV-B targets mainly the epidermis whilst UV-A radiation targets both epidermis and dermis (Vioux-Chagnoleau, *et al*., 2006; Quan, *et al*., 2004). Pigmented *Xenopus laevis* dorsal skin was exposed 5 min to a radiation of 6 J/cm^2 UV-B (312 nm). In Figure 3.4 it is possible to observe that the epidermis was the structure most damaged which is in agreement with what was previously described after UV-B exposure (Vioux-Chagnoleau, *et al*., 2006). The epidermis has a paramount importance avoiding cell damage and death. It was previously demonstrated that epidermal surviving cells can acquire gene mutations and genome instability and become unable of proper regulation of cell proliferation, leading eventually to cancer (Stout, *et al*., 2005; Ivanova, *et al*., 2005). In this respect, basal keratinocytes are considered crucial in the development of UV-induced skin tumours and apoptosis of keratinocytes is one of the typical biological markers of UV-B exposure (Stout, *et al*., 2005; Jans, *et al*., 2006).

Immediately after UV-B exposure (Figure 3.4b) no changes could be observed in the epidermis when compared with normal skin. In skin exposed to UV-B after 4 h in culture (Figure 3.3e) it was possible to observe a separation of the basal layer of epidermis and some cells from the interior layer of epidermis possibly underwent apoptosis which would clearly reflect a moderate sunburn reaction (Vioux-Chagnoleau, *et al*., 2006). Squamous cells loss observed in the epidermis correspond to regions where sunburned cells were previously located (indicated by arrow-heads in Figures 3.3e and 3.3f). This fact was already observed in several studies by IHC analysis using known apoptotic markers such as p53 protein and anti-caspase (Quan, *et al*., 2004; van Oosten, *et al*., 2000). Since IHC methods could not be performed due to technical problems the conclusions in this study were taken based only upon classical histology. It is a general consensus in dermatological science that epidermal turnover ensures a steady removal and renewal of epidermal cells that may have acquired damage avoiding skin deterioration (Stout, *et al*., 2005; Ivanova, *et al*., 2005). In this study (Figure 3.3f), epidermis turnover did not occur and the epidermis seems to have its interior layers degraded. The same changes were observed in Figure 3.4g after 12 h in culture with the increase that the upper and basal layers of epidermis were almost separated with the exception of regions containing secretory ducts.

Although UV-B was reported not to affect directly the dermis it can have some influence through indirect mechanisms involving the release of soluble factors by

keratinocytes. These mechanisms include enzymes that are responsible for tissue remodelling, degradation or modification of the extracellular matrix (collagen) which lead to a progressive degeneration of the dermis (Vioux-Chagnoleau, *et al*., 2006). Due to this, alterations of the components of the dermis after UV-B exposure were also evaluated. No noticeable changes were observed in the dermis of any samples. All gland modifications seem to be related with culture incubation times rather than with UV-B exposure. For instance after skin has been kept in culture for 4 h with (Figure 3.3e) or without UV-B exposure (Figure 3.4d) the mucous glands appear be closer to the epidermis and granular glands content seems not to be as compact. This was also observed in Figure 3.4f and Figure 3.4h, where mucous glands appear smaller and granular content was not compact.

The pigmentary defence against UV radiation will depend on the genetic inheritance of each individual (April and Barsh, 2007) and since this preliminary study was performed with only one individual no conclusion can be taken upon the average number, size or arrangement of chromatophores which could give an indication of the possible defence of individuals against the UV induced damage.

In previous studies, where electrophysiological parameters were evaluated it was concluded that frog skin UV-B irradiated within 1.0 J/cm^2 to 30 J/cm^2 has a tissue response to UV-B radiation (Leliñska, *et al*., 2005). Since the objective of this project was to evaluate changes in expression of PTH transcripts a value of UV-B irradiation within the described range would in theory induce a response. The value chosen was 6 J/cm^2 corresponding to 5 min exposure time. It seems that this value was appropriate given that it was observed a deterioration of the epidermis, a classical sign of a sunburn reaction (Vioux-Chagnoleau, *et al*., 2006). Although, this value can be appropriated to this individual, further studies have to be performed to validate the correct UV-B intensity to be used as a stressor in UV-B response. This step is of extreme importance since the effects of the UV radiation depend upon species and upon variations within populations (Leliñska, *et al*., 2005). For example in human the dosage can vary from 0.1 J/cm^2 to 40 J/cm2 provoking from solar urticaria to polymorphic light eruption, respectively (Leliñska, *et al*., 2005). Mice epidermis shows apoptotic cells 6 h after exposure of only 0.2 J/cm^2 UV-B light (van Oosten, *et al*., 2000). Also in mice a higher

value of UV-B (500 J/m2) for 2 min a day during 3 months leads to cancer formation with the first signs of epidermal apoptosis after 40 h (Jans, *et al*., 2006).

In human and other mammals, UV-exposure increases melanogenesis and this is the major protective skin response against photo-damage due to the ability of melanin to absorb damaging photons that target DNA (Goukassian, *et al*., 2004). The frog chromatophores are the amphibian equivalent of the human melanocytes involved in melanin production (Fingerman, 1965) and since albino frogs lack these structures the result of an UV exposure can be more devastating. Thus, the final experiment was performed with slightly less UV-B irradiation (4,8 J/cm^{2}with the intent of obtaining similar effects as the ones previously described for pigmented *Xenopus*. Moreover, final experiment was performed with skin 4 h in culture due to the fact that major changes in skin structure and morphology occur between 2 and 6 hours and are most probably associated with UV-B exposure.

The final UV-B experiment was performed using albino *Xenopus laevis* skin due to the unavailability of pigmented *Xenopus laevis*. Albino frog skin was also characterised prior to the experiments (Group A) and despite the fact that it was found to be much thinner and fragile there were no considerable differences in morphology (Figure 3.5) with the exception of the absence of chromatophores when compared to normal pigmented frogs (Figure 3.4). A very compact layer of epidermis stained red (Masson's trichrome staining) can be seen and mucous and granular glands are closer to the epidermis with shorter ducts (Figure 3.5).

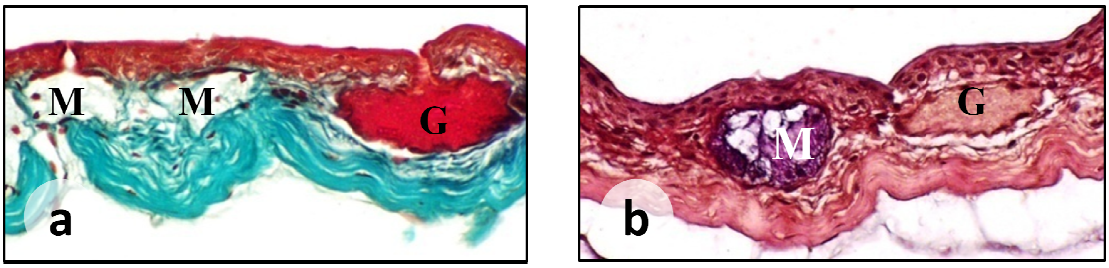

Figure 3.5 – Section through a young normal albino *Xenopus laevis* skin after staining with a) Masson´s trichrome and b) Alcian Blue [Amplification 20x]. (M - Mucous gland, G- Granular gland)

Skin explants taken from different individuals were exposed to UV-B and maintained in culture for 4 h (Group C) (Figure 3.6b and d)) or simply maintained in culture for 4 h (Group B) (Figure 3.6a and c) were analysed using Masson's trichrome and Alcian Blue staining.

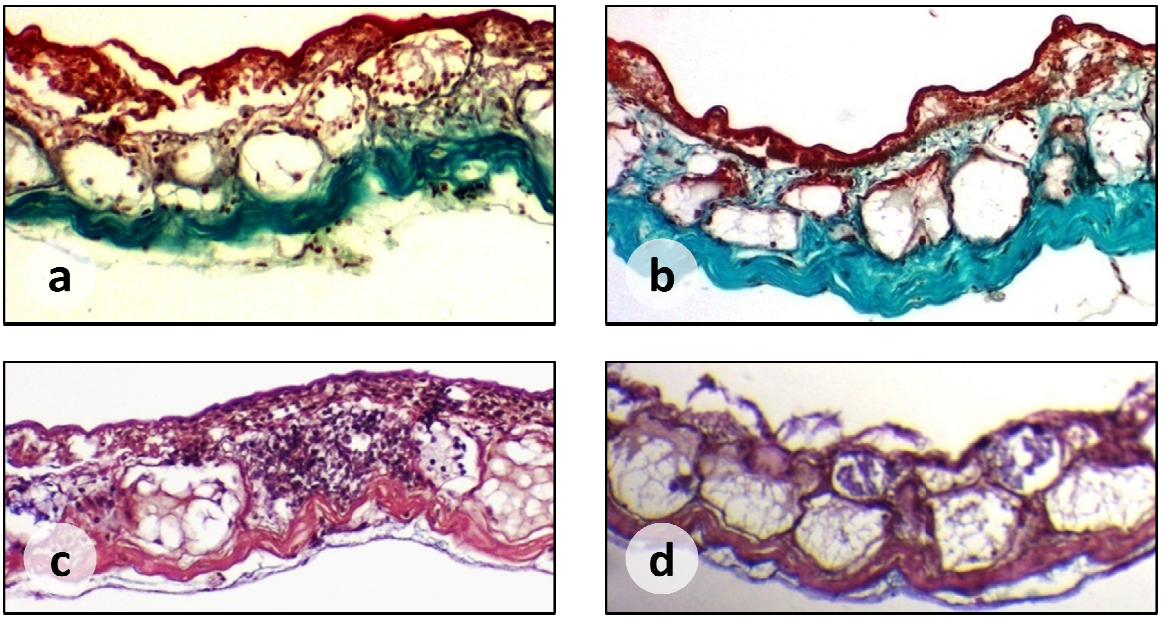

Figure 3.6 – Section through a young albino *Xenopus laevis* skin. (a and c) normal skin after media contact of 4 h and (b and d) UV exposure skin and media contact of 4 h after staining with (a and b) Masson´s trichrome and (c and d) Alcian Blue [Amplification 10x].

In Group B and in Group C considerable modifications occurred and significant loss of the integrity of the epidermis and dermis were observed when compared with Group A. Also, it was difficult to distinguish between granular and mucous glands despite the use of differential stains. The results of Masson's trichrome staining suggested that significant reorganisation occurred in the skin as collagen rich connective tissue appeared to be more abundant between glands in dermis and at the interface with the epidermis when compared with control (Figure 3.6). These observations are in agreement with previous studies where degradation of collagen reduces the viscosity and strength of dermis when supporting skin structure (Cooper, *et al*., 1965; Raab, 1970) and expression analysis of collagen will give a clearer picture of the changes observed.

Based only on the classical histology it was possible to conclude that culture time was too long for albino *Xenopus* skin and it was not possible to conclude if UV-B radiation had the same effect in skin morphology as previously observed for pigmented frogs. Therefore analysis on the expression of UV-B response biological markers could give an idea if there were any induced molecular changes due to UV-B exposure.

3.3 Molecular characterisation of UV response

In the present study, in order to determine the role of the PTH/PTHrP system in skin recovery or apoptosis the expression of PTH/PTHrP family members were determined

in normal and UV-B exposed skin of albino *Xenopus laevis*. UV radiation evokes local and systemic changes in skin function and their effect on different organisms depends not only on skin pigmentation and affected region but also on exposure length (Leliñska, *et al*., 2005). This was performed using three study groups (n=4): group A (normal skin), group B (control skin maintained in culture 4 h) and group C (skin UV-B exposed and maintained in culture 4 h). First, UV-B skin response was evaluated by using three biological markers involved in the formation of components of epidermis and dermis and in apoptotic processes. Human genes were used to find the *Xenopus* homologues in genomic databases and the chosen biological markers were keratin 8, Collagen type XVIII and p51/p63. A brief description of the selected genes can be found in Table 3.4.

Keratin 8 (BC044116) is described as a type II keratin, member of a family of intermediate filaments in epithelial cells (Watanabe, *et al*., 2001). Keratin 8 belongs to the differentiation-associated keratins that are expressed in the suprabasal cells of epidermis (Toftgard, *et al*., 1985). This protein was found to be a useful maker to characterize vertebrate epithelial cells because differential keratin expression has been demonstrated in malignant transformed epidermal cells (Jans, *et al*., 2006; Toftgard, *et al*., 1985). Furthermore, it was reviewed by Hoffmann (1984) that all human keratins have homologues in *Xenopus laevis* genome (Hoffmann, 1984). Therefore any modifications in keratin expression in frog can be related with what happens in human skin when exposed to UV-B.

Collagen is the major dermis component and was chosen as the second marker (collagen gene type XVIII (AY052763)). Collagen is described to be primarily synthesized by fibroblasts and proteolytically processed to form insoluble fibres. Disorganization, fragmentation, and dispersion of collagen are prominent features of photo-damaged human skin (Quan, *et al*., 2004) and therefore any modification in its expression can give an indication of UV-B induced damage.

Table 3.4 – Description of biological markers used to evaluate UV-B response.

Biological Marker	Description
Keratin 8 (cytokeratin 8, k8) (Toftgard, *et al*., 1985)	• Type II cytokeratin usually related with type I keratin 18. • Structural protein of the intermediate filament family mainly expressed in epithelial cells • Tightly linked to skin regeneration and differentiation. • Epidermal squamous cell carcinomas present an almost total loss of keratins transcripts related to differentiation. • Loss of differentiation-associated keratins was described as an early maker of malignant conversion
Collagen, type XVIII (col18A1) (Oofusa, *et al*., 1994; Myazaki, *et al*., 1996)	• Non-fibrillar collagen. • Contains the endostatin peptide that can be released after cleavage. • Most abundant on the basal layer of epithelial cells. • Functions on cell-matrix interaction. • Low turnover rate in normal tissues. • In metamorphosis, tail cells fall into programmed death and collagen expression is sharply repressed. • Degradation of collagens destabilises the differentiated state and is a trigger of tissue dedifferentiation.
p51/p63 (Tomimori, *et al*., 2004)	• Member of the tumour suppressor p53 gene family. • Produces at least 6 isotypes in human. • In human transactivator (TA) and N-terminal deleted (ΔN) isotypes can be found. • Regulates transcription of a variety of genes essential for skin development. • Possesses a DNA binding domain (DBD). • Only ΔN isotypes are so far found in *Xenopus laevis*. • TA isotypes accumulate and ΔN isotypes decrease their expression in response to DNA damage.

Since one of the main characteristics of UV-B response was described as the apoptosis of the epidermal cells the third and last marker chosen was an apoptotic marker, from the family of the tumour suppressor p53, the gene p51/p63 (AY459428.1). In mammals p51/p63 gene produces at least 6 isoforms. Three encode for a transactivator (TA) and three for an N-terminally deleted (ΔN) isoforms. Although the p51/p63 sequences are well conserved in humans and other vertebrates, only ΔN transcripts were so far identified in zebrafish and *Xenopus* (Lu, *et al*., 2006; Tomimori, *et al*., 2004). *Xenopus* ΔN p51/p63 isotypes have a conserved domain structure consisting of a DNA binding domain (DBD) and an oligomerization domain (OLID) (Tomimori, *et al*., 2004).

To have a general idea on the expression pattern of the biological markers chosen for expression studies *in silico* gene tissue distribution was evaluated using available EST expression data (Table 3.5).

Table 3.5 – *In silico* gene expression pattern of the biological markers chosen. ((√) indicates expression)

	brain	ectoderm	endomesoderm	eye	fat body	head	intestine	Keller explant	limb	lung	mesonephric kidney	oocyte	ovary	oviduct	oviduct stomach	skin	spleen	stomach	tail	testis	thymus	unfertilized egg	bone	heart
Keratin 8 (BC044116)	√	√	√	√	√	√	√	√	√	√	√	√	√	√		√	√	√	√	√	√	√		
Collagen, type XVIII (AY052763)	√	√		√		√		√	√		√				√	√				√			√	√
Tumour protein p51/p63 (AY459428.1)						√			√							√			√	√			√	

The tissue expression profile of the chosen biological markers and PTH related peptides (PTH-L, PTHrPA, and PTHrPB) can be found in Figure 3.7. Due to technical problems it was not possible to perform the expression studies of PTH precursor and of PTH/PTHrP receptors.

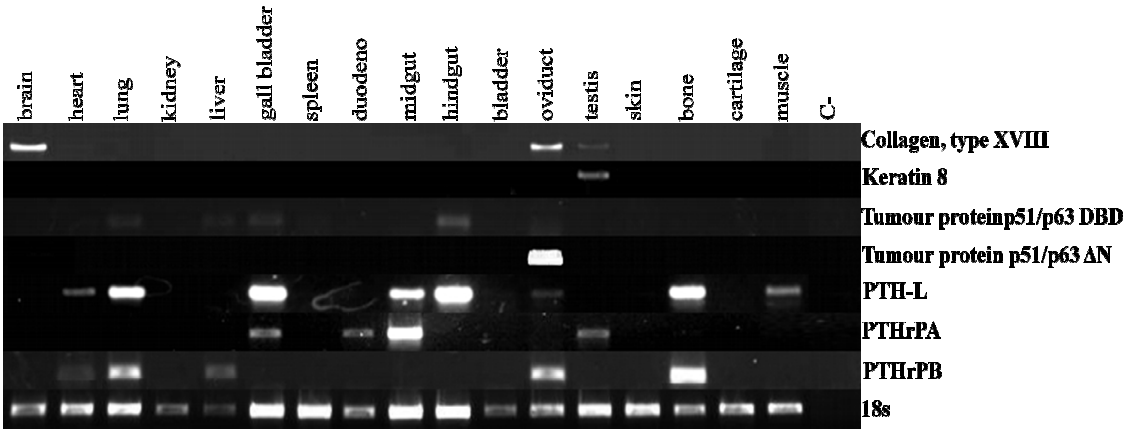

Figure 3.7 –Tissue expression of biological markers and PTH related peptides in pigmented *Xenopus laevis*. 18s expression was used as a control of cDNA amount.

Although, *in silico* expression profile indicated a wide distribution of keratin 8, this gene was only amplified from testis. Collagen (type XVIII) was found to be expressed in brain, testis and oviduct. Tissue expression of p51/p63 (ΔN region and DBD region) indicated that this gene was expressed in lung, gall bladder, hindgut, oviduct and liver.

In general, PTH/PTHrP family members have a widespread distribution in all analysed tissues and a possible function was given by Gomes (2007). PTH-L was found to be expressed in heart, lung, liver, midgut, hindgut, oviduct, bone and muscle. PTHrPA

isoform was expressed in the gall bladder, duodenum and testis and PTHrPB isoform was found in heart, lung, liver, oviduct and bone. The high expression of PTHrPB isoform in the oviduct and bone suggests a role in growth and cellular development as described before by Philbrick (1996). However, in contrast with previously reported PTH-L and PTHrPA isoform were found to be present in several tissues. Abnormally, no expression was observed in the skin sample used and the reason for this failure remains to be clarified since in preliminary studies performed in primer optimization the genes were successfully amplified in skin samples.

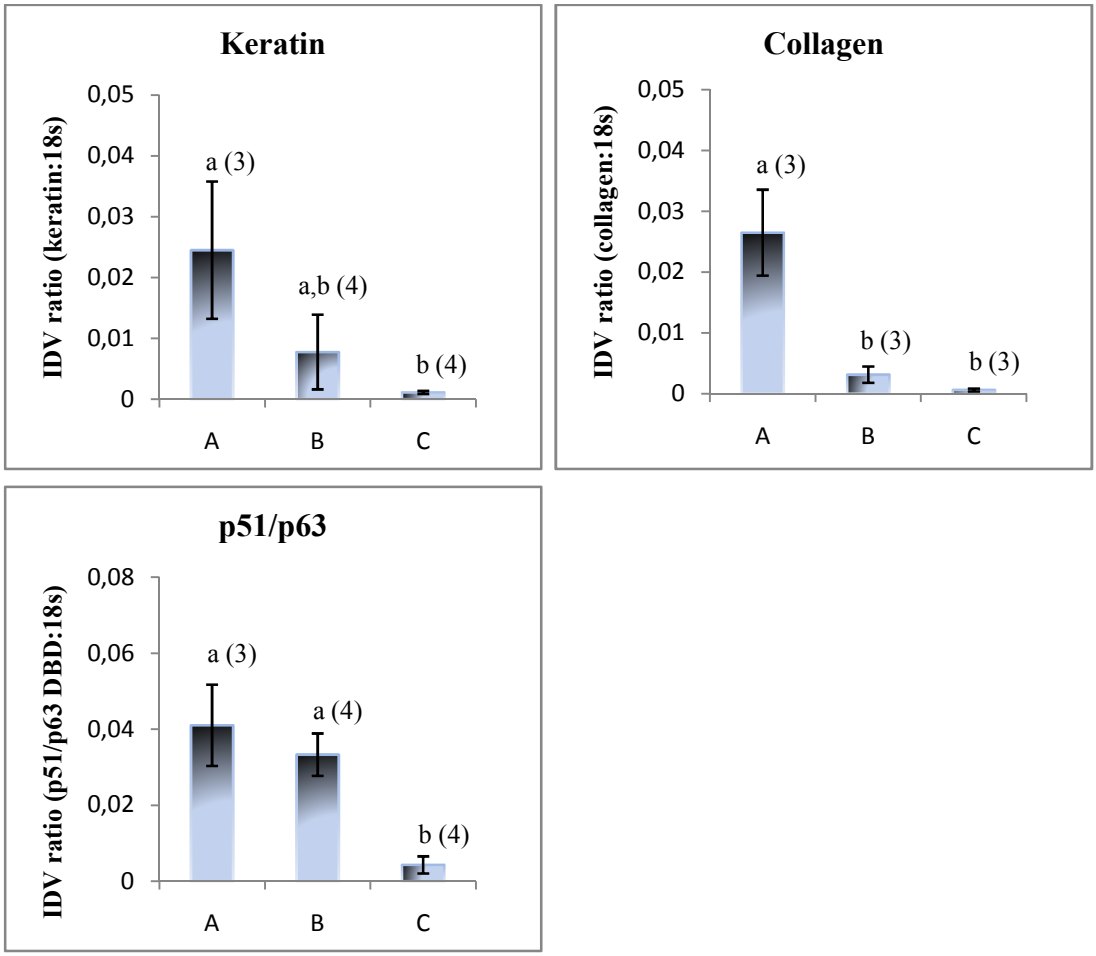

Figure 3.8 – Semi-quantitative expression assay performed to the 3 groups (n=4) of albino *Xenopus laevis* skin tested. Three biological markers: keratin 8, collagen type XVIII, and p51/p63 (DBD). Group A: normal skin; Group B: normal skin maintained in culture for 4 h; Group C: skin exposed to UV-B and maintained in culture for 4 h. IDV values were calculated using AlphaEase ®FC software (Alpha Innotech Corporation, USA).

Keratin 8 expression mean in group C (UV-B exposed cultured 4 h) decreased significantly compared to group A (normal). In agreement, previous studies performed with mouse keratin during skin carcinogenesis have shown a decrease of differentiation-associated keratins to 25% of control values 4 h after exposure (Toftgard, *et al*., 1985).

In order to verify if the observed decrease could be related with culture time, group B (cultured 4 h without UV-B exposure) was also accounted in this evaluation. If no change (up or down) was observed in the expression from group A to group B this would mean that the expression of keratin 8 was influenced by the UV-B exposure, in contrary a change in expression (up or down) would indicate that the medium used was affecting the expression of this gene. It was not possible to exclude the influence of culture time in keratin expression although a slight decrease of expression could be seen from group A to group B. This difference was found not to be statistically significant. Comparing group B with group C, the decrease of expression was also found not to be significant. A similar analysis should be performed with a larger number of individuals to evaluate if changes in keratin 8 expression are related only to UV-B exposure. This would suggest a change of normal epidermis differentiation since the decreased expression of differentiation-associated keratins is an early marker of malignant conversion (Klein-Szanto, *et al*., 1983).

Several changes have been reported to structural and biochemical parameters in mammal dermis upon UV exposure. The major component of the dermis (collagen) seems to play a crucial role in early events of UV response leading to the disorganization and progressive degeneration of skin structure (Vioux-Chagnoleau, *et al*., 2006). UV radiation disrupts skin collagen matrix by two interdependent pathways: stimulating collagen degradation and inhibiting collagen production (Quan, *et al*., 2004). However, since the UV range of radiation used was the UV-B and culture time was only four hours it was not expected a change in the expression of the collagen given that UV-B can only act on the dermis through indirect means (Vioux-Chagnoleau, *et al*., 2006). Therefore, when observing the differences of expression of collagen (Figure 3.8) it was surprising to find that a significant decrease of the expression occurred between the groups A (normal) and C (UV exposed cultured 4 h). The same significant decrease was observed from groups A (normal) to B (culture 4h). In this way it was possible to conclude that changes in collagen expression were related to culture time. This was corroborated by the classical histology (Figure 3.6) results where it was possible to observe a disorganization of collagen filaments on the stratum spongiosum of the dermis in groups B and C.

For p51/p63 gene it was possible to see a clear decrease in the expression in group A (normal) to C (UV exposed cultured 4h) and the same statistically significant decrease was observed for group B (cultured 4h) to C. Therefore, it was possible to distinguish that changes in expression were related to UV-B exposure and not to culture time. Consequently, the given stimulus induced DNA damage and subsequently decreased the expression of the p51/p63 gene as previously described by Tomimori (2004). This indicates that the provided UV-B radiation of 4.8 J/cm^2 and an exposure of 4 min were sufficient to induce an UV response and influences gene expression. In agreement to the obtained results in *Xenopus*, p51/p63 isoforms decrease their expression upon DNA damage (Tomimori, *et al*., 2004).

The expression of two PTH/PTHrP family members was also evaluated: PTHrPA and PTH-L (Figure 3.9). For PTHrPB isoform and PTH due to technical problems it was not possible to perform this semi-quantitative assay.

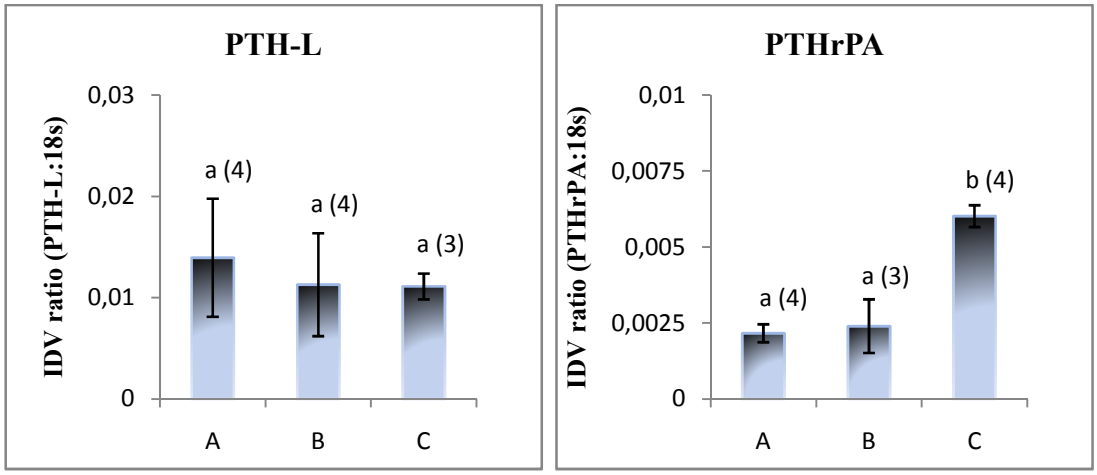

Figure 3.9 – Semi-quantitative expression assay performed to the 3 groups of albino *Xenopus laevis* skin tested. PTH transcripts: PTHrPA and PTH-L. (Group A: normal skin; Group B: normal skin maintained in culture for 4 h; Group C: skin exposed to UV-B and maintained in culture for 4 h). IDV values were calculated using AlphaEase ®FC software (Alpha Innotech Corporation, USA).

PTH-L expression remains basically constant in the three analysed groups therefore it seems not to be involved in UV-B response.

PTHrPA isoform mean expression significantly increases from group A to group C and from group B to C which indicates that this gene expression was up-regulated upon UV-B exposure. This is in agreement with previous reports where cultured medulloblasts glioma cells treated with hPTHrP reported to increase cell proliferation and decrease apoptosis (Gessi, et al., 2007), therefore some relation exists between PTHrPA isoform increased expression and UV-B induced response.

4. Conclusions

The aim of this study was to estimate possible roles of PTH/PTHrP family on cell proliferation, apoptosis and skin recovery related with UV-B response. The effect of UV-B radiation on pigmented and albino *Xenopus laevis* skin was first evaluated using classical histology. This revealed high modification in the epidermis between 2 h and 6 h after exposure. Furthermore, it was possible to observe epidermis degradation which might be due to apoptosis of keratinocytes within the supra-basal layers of epidermis and to the lack of epidermis turnover in pigmented *Xenopus* skin. The observation of albino *Xenopus* skin through classical histology did not allow concluding about the effect of UV-B radiation since significant reorganization of skin structure occurred in cultured normal skin and in UV-B exposed skin. UV-B induced damage was also evaluated using UV-B response biological markers (keratin 8, collagen type XVIII and p51/p63). The evaluation of p51/p63 gene expression permitted to confirm the conclusions taken by classical histology that UV-B radiation induced apoptosis of skin cells. Changes in expression of PTH/PTHrP family members were also evaluated. PTH-L expression does not seem to be influenced by UV-B radiation and PTHrPA isoform appears to have a role in UV-B response (e.g. skin regeneration, apoptosis, etc...).

5. Future work

In this study, although it was possible to induce UV-B response some alterations on the methods can be performed:

- A new PCR, isolation and sequencing should be made on the predicted PTH2R first exon. Also, alternative methods (e. g. RACE 5' regions) can be used to determine the missing receptor sequences.
- Although some IHC tests have been done they were not successful since albino frog skin was very fragile and did endure the method. These trials could be repeated with adult albino frogs or with normal pigmented *Xenopus laevis*.
- If trials are to be continued with albino *Xenopus laevis* then a change in the culture medium is advised since the skin presented reorganization after 4 h in culture without UV exposure;
- The modifications on gene expression of all genes can be evaluated quantitatively by real time PCR since this semi-quantitative assay does not take into account PCR efficiency;
- A further characterisation of the UV-B response can be made using antibodies to detect apoptotic epidermal cells, namely the anti-caspase 3 antibody or a widely studied apoptotic marker, tumour protein p53;
- Also an antibody could be used to determine UV-B indirect effects on the dermis (e. g. MMP-1). MMP-1 antibody is a protein that increases its expression upon UV-B radiation.

6. References

Abbink, W. and Flik, G. (2006). Parathyroid Hormone-related Protein in Teleost Fish. *General and Comparative Endocrinology , 152* (2-3), 243-251.

April, C.S. and Barsh, G.S. (2007). Distinct Pigmentary and Melanocortin 1 Receptor–dependent Components of Cutaneous Defense against Ultraviolet Radiation. *Public Library of Science Genetics , 3* (1), 30-43.

Bergwitz, C., Klein, P., Kohno, H., Forman, S., Lee, K., Rubin, D., *et al.* (1998). Identification, Functional Characterization, and Developmental Expression of Two Nonallelic Parathyroid Hormone (PTH)/PTH-Related Peptide Receptor Isoforms in Xenopus laevis (Daudin). *Endocrinology , 139* (2), 723-732.

Bjarnadóttir, T., Gloriam, D., Hellstrand, S., Kristiansson, H., Fredriksson, R. and Schiöth, H. (2006). Comprehensive Repertoire and Phylogenetic Analysis of the G Protein-coupled Receptors in Human and Mouse. *Genomics , 88* (3), 263-273.

Brewer Jr., H. B., Fairwell, T., Ronan, R., Sizemore, G. W., and Arnaud, C. D. (1972). Human Parathyroid Hormone: Amino-Acid Sequence of the Amino-Terminal Residues 1-34. *Proceedings of the National Academy of Sciences , 69* (12), 3585-3588.

Brown, E. M. (2000). The Extracellular Ca2+ - Sensing Receptor: Central Mediator of Systemic Calcium Homeostasis. *Annual Review of Nutrition , 20*, 507-533.

Campbell, N., and Reece, J. B. (2005). *Biology* (7th ed.). San Francisco: Addison-Wesley.

Canario, A. V., Rotllant, J., Fuentes, J., Guerreiro, P. M., Teodosio, R., Power, D. M., *et al.* (2006). Novel Bioactive Parathyroid Hormone and Related Peptides in Teleost Fish. *Federation of European Biochemical Societies Letters , 580* (1), 291-299.

Clemens, T. L., Cormier, S., Eichinger, A., Endlich, K., Fiaschi-Taesch, N., Fischer, E., *et al.* (2001). Parathyroid Hormone-Related Protein and its Receptors: Nuclear Functions and Roles in the Renal and Cardiovascular Systems, the placental trophoblasts and the Pancreatic Islets. *British Journal of Pharmacology , 134* (6), 1113-1136.

Danks, J. A., Martin, T. J. and Ingleton, P. M. (1997). Parathyroid Hormone-related Protein in Tissues of the Emerging Frog (Rana temporaria): Immunohistochemistry and in Situ Hybridisation. *Journal of Anatomy , 190*, 229-238.

Danks, J. A., Ho, P., Notini, A. J., Katsis, F., Hoffmann, P., Kemp, B. E., *et al.* (2003). Identification of a Parathyroid Hormone in the Fish Fugu rubripes. *Journal of Bone and Mineral Research , 18* (7), 1326-1331.

Fox, S. I. (1996). *Human Physiology* (5th ed.). Dubuque : William. C. Brown Publishers.

Gensure, R. C., Gardella, T. J. and Juppner, H. (2005). Parathyroid Hormone and Parathyroid Hormone-related Peptide, and their Receptors. *Biochemical and Biophysical Research Communications , 328* (3), 666-678.

Gensure, R. C., Ponugoti, P., Gunes, Y., Papasani, M. R., Lanske, B., Bastepe, M., *et al.* (2004). Identification and Characterization of Two Parathyroid Hormone-Like Molecules in Zebrafish. *Endocrinology , 145* (4), 1634-1639.

Gomes, A. (2007). *Caracterização Molecular e Funcional dos Sistemas PTH/PTHrP em Anfíbios.* Relatório de Estágio de Licenciatura, Universidade do Algarve, Faculdade de Ciencias e Tecnologia.

Goukassian, D. A., Helms, E., van Steeg, H., van Oostrom, C. and Bhawan, J. (2004). Topical DNA Oligonucleotide Therapy Reduces UV-induced Mutations and Photocarcinogenesis in Hairless Mice. *Proceedings of the National Academy of Sciences , 101* (11), 3933-3938.

Guerreiro, P. M., Renfro, J. L., Power, D. M. and Canario, A. V. (2007). The Parathyroid Hormone Family of Peptides: Structure, Tissue Distribution, Regulation, and Potential Functional roles in Calcium and Phosphate Balance in Fish. *American Journal of Physiology - Regulatory, Integrative, and Comparative Physiology , 292*, R679-R696.

Habener, J. F., Potts Jr., J. T. and Rich, A. (1976). re-Proparathyroid Hormone - Evidence for an Early Biosynthetic Precursor of Proparathyroid Hormone. *The Journal of Biological Chemistry , 251* (13), 3893-3899.

Harmar, A. J. (2001). Family-B G-protein-coupled receptors. *Genome Biology , 2* (12), 1-10.

Heinrich, G., Kronenbergs, H. M., Potts Jr, H. T. and Habener, J. F. (1984). Gene Encoding Parathyroid Hormone - Nucleotide Sequence of the Rat Gene and Deduced Amino Acid Sequence of Rat. *The Journal of Biological Chemistry , 259* (5), 3320-3329.

Henderson, J. E., Kremer, R., Rhim, J. S. and Goltzman, D. (1992). Identification and Functional Characterization of Adenylate Cyclase-Linked Receptors for Parathyroid

Hormone-Like Peptides on Immortalized Human Keratinocytes. *Endocrinology , 130* (1), 449-457.

Hermans, E. (2003). Biochemical and Pharmacological Control of the Multiplicity of Coupling at G-protein-coupled Receptors. *Pharmacology & Therapeutics , 99* (1), 25-44.

Hoare, S. and Usdin, T. (2001). Molecular Mechanisms of Ligand Recognition by Parathyroid Hormone 1 (PTH1) and PTH2 Receptors. *Current Pharmaceutical Design , 7*, 689-713.

Ingleton, P. M. (2002). Parathyroid Hormone-Related Protein in Lower Vertebrates. *Comparative Biochemistry and Physiology, Part B , 132* (1), 87-95.

Ingleton, P. M. and Danks, J. A. (1996). Distribution and Functions of Parathyroid Hormone-related Protein in Vertebrate Cells. *International Review of Cytology , 166*, 231-280.

Ivanova, I. A., D'Souza, S. J., & Dagnino, L. (2005). Signalling In The Epidermis: The E2f Cell Cycle Regulatory Pathway In Epidermal Morphogenesis, Regeneration And Transformation. *International Journal of Biological Sciences , 1*, 87-95.

Jans, J., Garinis, G. A., Schul, W., van Oudenaren, A., Moorhouse, M., Smid, M., *et al.* (2006). Differential Role of Basal Keratinocytes in UV-Induced Immunosuppression and Skin Cancer. *Molecular and Celular Biology , 26* (22), 8515-8526.

Joun, H., Lanske, B., Karperien, M., Qian, F., Defize, L., Abou-Samra, A. (1997). Tissue-specific Transcription Start Sites and Alternative Splicing of the Parathyroid Hormone (PTH)/PTH-related Peptide (PTHrP) Receptor Gene: a New PTH/PTHrP Receptor Splice Variant that Lacks the Signal Peptide. *Endocrinology , 138*, 1742–1749.

Juppner, H., Abou-Samra, A., Freeman, M., Kong, X. F., Schipani, E., Richards, J., *et al*. (2001). A G Protein-Linked Receptor for Parathyroid Hormone and Parathyroid Hormone-Related Peptide. *Science , 254* (5034), 1024-1026.

Kardong, K. V. (1998). *Vertebrates: Comparative Anatomy, Function, Evolution* (2th ed.). Dubuque: William C. Brown/ McGraw-Hill.

Kremer, R., Karaplis, A. C., Henderson, J., Gijlliver, W., Banville, D., Hendy, G. N., *et al.* (1991). Regulation of Parathyroid Hormone-like Peptide in Cultured Normal Human Keratinocytes. *The Journal of Clinical Investigation , 87* (3), 884-893.

Kroeze, W. K., Sheffler, D. J. and Roth, B. L. (2003). G-protein-coupled Receptors at a Glance. *Journal of Cell Science , 116* (Pt 24), 4867-4869.

Lavine, J. A., Rowatt, A. J., Klimova, T., J., W. A., Dengle, E., Beck, C., *et al.* (2005). Aryl Hydrocarbon Receptors in the Frog Xenopus laevis: Two AHR1 Paralogs Exhibit Low Affinity for 2,3,7,8-tetrachlorodibenzop-p-dioxin (TCDD). *Toxicological Sciences , 88* (1), 60-72.

Leliñska, A., Zegarska, B., Meodzik-Danielewicz, N., Kaczorowski, P. and Tyrakowski, T. (2005). Influence of UV Radiation on Electrophysiological Parameters. *Zoologica Poloniae , 50* (4), 87-106.

Mackenna, B. R. and Callander, R. (1997). *Illustrated Physiology* (6th ed.). New York: Churchill Livingstone.

Madson, J. G., Lynch, D. T., Tinkum, K. L., Putta, S. K. and Hansen, L. (2006). Erbb2 Regulates Inflammation and Proliferation in the Skin after Ultraviolet Irradiation. *The American Journal of Pathology , 169* (4), 2408-2412.

Mangin, M., Ikeda, K., Dreyer, B. and Broadus, A. (1989). Isolation and Characterisation of the Human Parathyroid Hormone-like Peptide Gene. *Procedures of the National Academy of Sciences , 86* (7), 2408-2412.

Merendino, J., Insogna, K., Milstone, L., Broadus, A. and Stewart, A. (1986). A Parathyroid Hormone-like Protein from Cultured Human Keratinocytes. *Science , 231* (4736), 388-390.

Moseley, J. M., Kubota, M., Diefenbach-Jagger, H., Wettenhall, R. E., Kemp, B. E., Suva, L. J., *et al.* (1987). Parathyroid Hormone-related Protein Purified from a Human Lung. *Procedures of the National Academy of Sciences , 84* (14), 5048-5052.

Myazaki, K., Uchiyama, R. I. and Yoshizato, K. (1996). Cloning and Characterization of cDNAs for Matrix Metalloproteinases of Regenerating Newt Limbs. *Procedures of the National Academy of Sciences , 93* (13), 6819-6824.

Oofusa, K., Yomori, S. and Yoshizato, K. (1994). Regionally and Hormonally Regulated Expression of Genes of Collagen and Collagenase in the Anuran Larval Skin. *International Journal of Developmental Biology , 38* (2), 345-350.

Orloff, J., Kats, Y., Mitnick, M., Gasalla-Herraiz, J. and Isales, C. M. (1993). Evidence for a Receptor on Squamous Carcinoma Cell Lines which Recognizes a Mid-region Fragment of Parathyroid Hormone-related Protein, PTHrP(67-86)NH2. *Journal of Bone and Mineral Research , 8* (Suppl 1), S133.

Philbrick, W. M., Wysolmerski, J. J., Galbraith, S., Holt, E., Orloff, J. J., Yang, K. H., *et al.* (1996). Physiology, Defining the Roles of Parathyroid Hormone-Related Protein in Normal Physiology. *Physiological Reviews , 76* (1), 127-73.

Potts, J. T. (2005). Parathyroid Hormone: Past and Present. *Journal of Endocrinology , 187* (3), 311-325.

Power, D. M., Ingleton, P. M., Flanagan, J., Canario, A. V., Danks, J., Elgar, G., *et al.* (2000). Genomic Structure and Expression of Parathyroid Hormone-related Protein Gene (PTHrP) in a Teleost, Fugu rubripes. *Gene , 250* (1-2), 67-76.

Quan, T., He, T., Kang, S., Voorhees, J. J. and Fisher, G. J. (2004). Solar Ultraviolet Irradiation Reduces Collagen in Photoaged Human Skin by Blocking Transforming Growth Factor-Type II Receptor/Smad Signaling. *American Journal of Pathology , 165* (3), 741-750.

Rolz, C., Pellegrini, M. and Mierke, D. F. (1999). Molecular Characterization of the Receptor-Ligand Complex for Parathyroid Hormone. *Biochemistry , 38* (20), 6397-6405.

Runge, S., Wulf, B. S., Madsen, K., Brauner-Osborne, H. and Knudsen, L. B. (2003). Diferent Domains of the Glucagon and Glucagon-like Peptide-1 Receptors Provide the Critical Determinants of Ligand Electivity. *British Journal of Pharmacology , 138* (5), 787-794.

Sartor, M. A., Zorn, A. M., Schwanekamp, J. A., Halbleib, D., Karyala, S., Howell, M. L., et al. (2006). A New Method to Remove Hybridization Bias for Interspecies Comparison of Global Gene Expression Profiles Uncovers an Association Between mRNA Sequence Divergence and Differential Gene Expression in Xenopus. *Nucleic Acids Research , 34* (1), 185-200.

Schreiber, A. M. and Brown, D. D. (2003). Tadpole Skin Dies Autonomously in Response to Thyroid Hormone at Metamorphosis. *Proceedings of the National Academy of Sciences , 100* (4), 1769-1774.

Slominski, A., Fischer, T. W., Zmijewski, M. A., Wortsman, J., Semak, I., Zbytek, B., et al. (2005). On the Role of Melatonin in Skin Physiology and Pathology. *Endocrine , 27* (2), 137-148. (Ivanova, et al., 2005)

Soifer, N. E., Dee, K. E., Insogna, K. L., Burtis, W. J., Matovcik, L. M., Wu, T. L., *et al.* (1992). Parathyroid Hormone-related Protein. Evidence for Secretion of a Novel Mid-region Fragment by Three Different Cell Types. *Journal of Biological Chemistry , 267* (25), 18236-18243.

Stiffler, D. F., Yee, J. C. and Tefft, J. D. (1998). Responses of Frog Skin, Rana pipiens, Calcium Ion Transport to Parathyroid Hormone, Calcitonin, and Vitamin D3. *General and Comparative Endocrinology , 112* (2), 191-199.

Suarez, F., Lebrun, J., Lecossier, D., Escoubet, B., Coureau, C. and Silve, C. (1995). Expression and Modulation of the Parathyroid Hormone (PTH)/PTH-related Peptide Receptor Messenger Ribonucleic Acid in Skin Fibroblasts from Patients with Type Ib Pseudohypoparathyroidism. *Journal of Clinical Endocrinology and Metabolism , 80*, 965-970.

Thompson, J. G. (1997). The ClustalX Windows Interface: Flexible Strategies for Multiple Sequence. *Nucleic Acids Research , 25* (24), 4876-4882.

Toftgard, R., Yuspa, S. H. and Roop, D. R. (1985). Keratin Gene Expression in Mouse Skin Tumors and in Mouse Skin Treated with 12-O-Tetradecanoy Iphorbol-13-acetate. *Cancer Research , 45* (11 Pt 2), 5845-5850.

Tortora, G. J. and Grabowski, S. R. (1996). *Principles of Anatomy and Physiology* (8th ed.). Menlo Park: Biological Sciences Textbooks, Inc.

van Oosten, M., Rebel, H., Friedberg, E. C., van Steeg, H., van der Horst, G. T., van Kranen, H. J., *et al.* (2000). Differential Role of Transcription-coupled Repair in UVB-induced G2 Arrest and Apoptosis in Mouse Epidermis. *Proceedings of the National Academy of Sciences , 97* (21), 11268–11273.

Vander, A., Sherman, J. S. and Luciano, D. S. (1985). *Human Physiology - The Mechanisms of Body Function* (4th ed.). New York: McGraw-Hill Book Company.

Vioux-Chagnoleau, C., Lejeune, F., Sok, J., Pierrard, C., Marionnet, C. and Bernerd, F. (2006). Reconstructed Human skin: From Photodamage to Sunscreen Photoprotection and Anti-aging Molecules. *Journal of Dermatological Science , 2* (1), S1—S12.

Winger, B. D. (1994). *The Human Body - Concepts of Anatomy and Physiology* (1th ed.). Forth Worth: Saunders College Publishing.

Yergeau, D. A. and Mead, P. E. (2007). Manipulating the Xenopus Genome with Transposable Elements. *Genome Biology , 8* (Suppl 1), 1-11.

Annexes

Annex I: Reagents, buffers and media

- **0.5% periodic acid:** 0,5 g periodic acid; dH_2O ad 100 ml
- **1x PBS:** 8.0 g NaCl; 0,2 g KH_2PO_4; 1.45 g $Na_2HPO_4.2H_2O$; 0.2 g KCl; 0.2 g NaN_3
- **10x OPA buffer:** 100 mM Tris acetate pH 7,5; 100 mM Magnesium acetate; 500 mM potassium acetate; H_2O ad 10 ml
- **1% Acid/Alcohol:** 1% (v/v)concentrated HCl, 70% Ethanol, 29% H_2O
- **1%-1.4% agarose gel:** 1-1.5 g agarose; 3 µl Ethidium bromide; 100 ml TAE-buffer
- **2% (v/v) APES:** 3-aminopropyltriethoxysilane in acetone
- **3% Glacial acetic acid:** 3 mL **a**cetic acid; dH_2O ad 100 mL
- **4%PFA:** 40g PFA; 100µl NaOH; 100 ml sterile 1M phosphate buffer (pH 7.4); dH_2O ad 900 mL
- **Alcian Blue Solution:** 100 mL 3% glacial acetic acid; 1 g Alcian Blue 8GX
- **DEPC water:** 200 µL of diethyl pyrocarbonate; dH_2O ad 2 L
- **Gill's Haematoxilin:** 2 g Haematoxilin add 250 mL ethylene glycol; 20 g aluminium sulphate; 20 mL Glacial acetic acid; 0,2 g sodium iodate; H_2O add 750 ml;
- **GTE:** 50 mM glucose; 10 mM EDTA; 25 mM Tris-HCl; pH 8.0; (0.1mg/ml RNase)
- **Harry's Haematoxilin:** 2,5 g Haematoxilin add 25 mL ethanol; 50 g potassium aluminium sulphate.$12H_2O$ add 500 ml H_2O; 1,25 g Red HgO; 20 mL Glacial acetic acid;
- **Eosin Y:** 1 g Eosin Y; dH_2O ad 100 mL
- **K-acetate solution:** 3 M KAc, pH 5.0
- **LB medium:** 4 tablets LB broth (Sigma)l; H_2O ad 200 mL
- **Loading buffer:** 40% Glucose ad 100 ml; 0,25 % Bromophenol blue
- **Lysis buffer:** 10 mM Tris-HCl, 400 mM NaCl in 2mM EDTA, pH 8.2
- **LB agar:** 8 LB agar tablets (Sigma); H_2O ad 400 mL
- **Mayer's Haematoxilin:** 1g Haematoxylin; 50 g aluminum potassium alum; 0,2 g sodium iodate; 20 ml glacial acetic acid; dH_2O ad 1000 mL
- **NaOH/SDS:** 0.2 M NaOH; 1% SDS
- **Phosphate buffer 1M (pH 7.4):** 31,15 g $Na_2HPO_4.2H_2O$; 11,70 $NaH_2PO_4.2H_2O$; H_2O ad 250 mL
- **SCHIFF's reagent:** 10 g basic fuchsin; 18 g sodium metabisulfite; 10mL Hydrochloric acid; dH_2O ad 1000 mL
- **SOB medium:** 2% Bacto tryptone; 1,5% yeast extract; 10 mM NaCl; 2,5 mM KCl; 10 mM $MgCl_2$; 10 mM $MgSO_4$
- **TAE buffer:** 40 mM Tris; 1 mM Na_2EDTA; 5 mM NaAc; pH 8.0
- **Transformation buffer (TB) (pH 6,7):** 10 mM Pipes; 15 mM CaCl2; 250 mM KCl
- **Wash buffer:** 10 mM Tris-HCl pH 8.0; 1 mM EDTA
- **Xylidine Ponceau:** equal volumes of 0.5% xylidine ponceau in 1% acetic acid and 0.5% acid fuchsin in 1% acetic acid;

Annex II: Primers

Name	Sequence (5' to 3')	T_m (^oC)
18s Fwd	TCA AGA ACG AAA GTC GGA GG	60
18s Rev	GGA CAT CTA AGG GCA TCA CA	60
XenEcoRIPTHR1Fwd	GCC GGG AAT TCG TGG ATG CTG ATG AT	70
XenXhoIPTHR1Rev	CTC GAG TTA CAT GAC AGT TTC TCT	76
XenBluntPTHR1Fwd	AAG TGG ATG CTG ATG ATG TCA	62
XenBluntPTHR1Rev	TTA CAT GAC AGT TTC TCT TTC TTC	64
XenEcoRIPTHR2Fwd	CCC GGG AAT TCG TTG ATT CTG ATG	72
XenXhoIPTHR2Rev	CTC GAG TAT AAA GTT TCC TCT ATT A	70
XenBluntPTHR2Fwd	AAG TTG ATT CTG ATG ATA CAG TT	60
XenBluntPTHR2Rev	CTA TAA AGT TTC CTC TAT TAC ATT	60
XenΔNp51/p63Fwd	GTA TCT GGA AAA CAA TGC TCA GG	66
XenΔNp51/p63Rev	TCA GCT CAT GAT TCG GAC AAC	62
XenDBDp51/p63Fwd	GGT TGT GAA GCG TTG TCC GA	62
XenDBDp51/p63Rev	GTG AAT TCC GTA CCC ACC TG	62
XenCollagenXIIIFwd	GTG TAT ATC GGG GTG AAG CT	60
XenCollagenXIIIRev	CTC TTT CTC CAC AGG GGT TC	62
XenKeratin8Fwd	ATG GCG AGT AGA GCC AGC	66
XenKeratin8Rev	TTC TCT AGC TCT GTG CGT CTG	64
XenXB-CadherinFwd	CAG ATG GCA CTG TCC TAG TAA	62
XenXB-CadherinRev	GAT CCT CTG AAC ACA GGC TG	62
XenMMPL1Fwd1	CCT CGA TGT GGT ATT GCT GA	60
XenMMPL1Rev1	ATG GTT CAG CAG GCT TTG TC	60
Xenp53Fwd1	GCC AGT TGG CCA AGA CTT	64
Xenp53Rev1	ATC ATC AAC AAC AAG ACG CTT C	62
Xenpthr1intFwd	GCG AAT TAT ACA GAG TGT CCA	60
Xenpthr1intRev	TAC TAT ATA GTT GGA CTC CAA A	58
Xenpthr2intFwd	TTG CAC TGC ACC AGG AAC TA	60
Xenpthr2intRev	ATT TTA GTT GCA ACA ACC CGC	58

Annex III – PTH/PTHrP receptors in vertebrates.

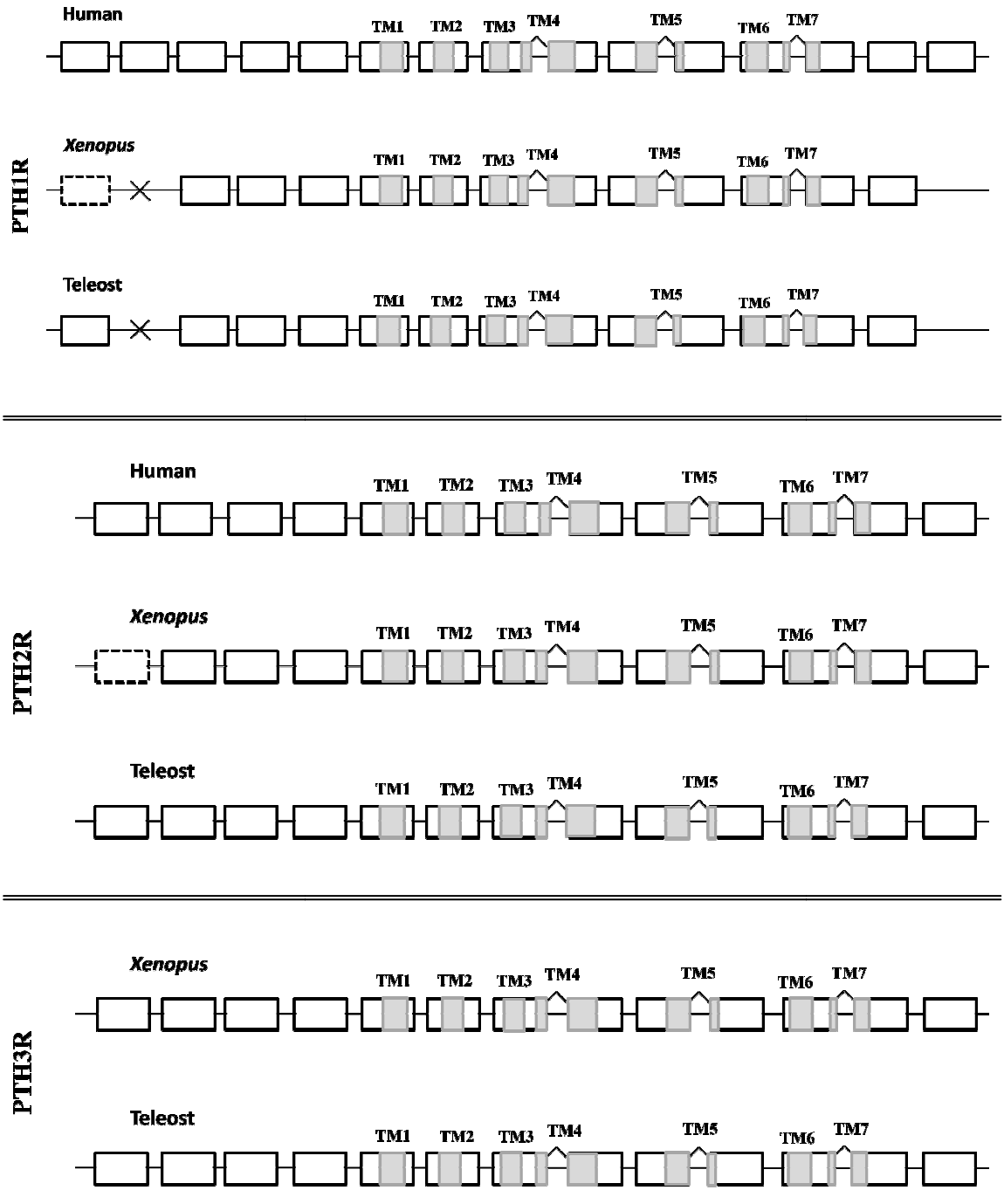

Annex IV – Statistical analysis

(Groups A, B and C referred in the main text are reported here as Groups 1, 2 and 3, respectively)

Univariate Analysis of Variance: Keratin

Between-Subjects Factors

		N
Groups	1	3
	2	4
	3	4

Tests of Between-Subjects Effects

Dependent Variable: Keratin

Source	Type III Sum of Squares	df	Mean Square	F	Sig.
Corrected Model	,002[a]	2	,001	5,687	,029
Intercept	,002	1	,002	16,120	,004
Groups	,002	2	,001	5,687	,029
Error	,001	8	,000		
Total	,005	11			
Corrected Total	,003	10			

a. R Squared = ,587 (Adjusted R Squared = ,484)

Post Hoc Tests

Multiple Comparisons

Keratin: Tukey HSD

(I) Groups	(J) Groups	Mean Difference (I-J)	Std. Error	Sig.	95% Confidence Interval Lower Bound	95% Confidence Interval Upper Bound
1,000	2,000	,02126	,009426	,121	-,00568	,04819
	3,000	,03154*	,009426	,025	,00461	,05848
2,000	1,000	-,02126	,009426	,121	-,04819	,00568
	3,000	,01029	,008726	,497	-,01465	,03522
3,000	1,000	-,03154*	,009426	,025	-,05848	-,00461
	2,000	-,01029	,008726	,497	-,03522	,01465

Based on observed means.

The error term is Mean Square(Error) = ,000.

*. The mean difference is significant at the 0,05 level.

Univariate Analysis of Variance: Collagen

Between-Subjects Factors

		N
Groups	1,000	3
	2,000	3
	3,000	3

Tests of Between-Subjects Effects

Dependent Variable: Collagen

Source	Type III Sum of Squares	df	Mean Square	F	Sig.
Corrected Model	,001[a]	2	,001	11,784	,008
Intercept	,001	1	,001	17,651	,006
Groups	,001	2	,001	11,784	,008
Error	,000	6	5,189E-5		
Total	,002	9			
Corrected Total	,002	8			

a. R Squared = ,797 (Adjusted R Squared = ,729)

Post Hoc Tests

Multiple Comparisons

Collagen: Tukey HSD

(I) Groups	(J) Groups	Mean Difference (I-J)	Std. Error	Sig.	95% Confidence Interval Lower Bound	95% Confidence Interval Upper Bound
1,000	2,000	,02337*	,005882	,017	,00532	,04141
	3,000	,02590*	,005882	,011	,00785	,04394
2,000	1,000	-,02337*	,005882	,017	-,04141	-,00532
	3,000	,00253	,005882	,905	-,01552	,02057
3,000	1,000	-,02590*	,005882	,011	-,04394	-,00785
	2,000	-,00253	,005882	,905	-,02057	,01552

Based on observed means.

The error term is Mean Square(Error) = 5,19E-005.

*. The mean difference is significant at the 0,05 level.

Univariate Analysis of Variance: p51/p63

Between-Subjects Factors

		N
Groups	1,000	3
	2,000	4
	3,000	4

Tests of Between-Subjects Effects

Dependent Variable: p51/p63

Source	Type III Sum of Squares	df	Mean Square	F	Sig.
Corrected Model	,002[a]	2	,001	7,393	,015
Intercept	,006	1	,006	44,917	,000
Groups	,002	2	,001	7,393	,015
Error	,001	8	,000		
Total	,009	11			
Corrected Total	,003	10			

a. R Squared = ,649 (Adjusted R Squared = ,561)

Post Hoc Tests

Multiple Comparisons

p51/p63: Tukey HSD

(I) Groups	(J) Groups	Mean Difference (I-J)	Std. Error	Sig.	95% Confidence Interval Lower Bound	95% Confidence Interval Upper Bound
1,000	2,000	,00559	,009039	,814	-,02023	,03142
	3,000	,03135*	,009039	,021	,00552	,05718
2,000	1,000	-,00559	,009039	,814	-,03142	,02023
	3,000	,02575*	,008369	,036	,00184	,04967
3,000	1,000	-,03135*	,009039	,021	-,05718	-,00552
	2,000	-,02575*	,008369	,036	-,04967	-,00184

Based on observed means.

The error term is Mean Square(Error) = ,000.

*. The mean difference is significant at the 0,05 level.

Univariate Analysis of Variance: PTH-L

Between-Subjects Factors

		N
Groups	1,000	4
	2,000	4
	3,000	3

Tests of Between-Subjects Effects

Dependent Variable: PTHL

Source	Type III Sum of Squares	df	Mean Square	F	Sig.
Corrected Model	,000[a]	2	5,811E-5	,639	,553
Intercept	,002	1	,002	22,185	,002
Groups	,000	2	5,811E-5	,639	,553
Error	,001	8	9,095E-5		
Total	,003	11			
Corrected Total	,001	10			

a. R Squared = ,138 (Adjusted R Squared = -,078)

Post Hoc Tests

Groups

Multiple Comparisons

PTHL: Tukey HSD

(I) Groups	(J) Groups	Mean Difference (I-J)	Std. Error	Sig.	95% Confidence Interval Lower Bound	Upper Bound
1,000	2,000	,00570	,006743	,688	-,01357	,02496
	3,000	,00770	,007284	,565	-,01311	,02851
2,000	1,000	-,00570	,006743	,688	-,02496	,01357
	3,000	,00200	,007284	,959	-,01881	,02282
3,000	1,000	-,00770	,007284	,565	-,02851	,01311
	2,000	-,00200	,007284	,959	-,02282	,01881

Based on observed means.

The error term is Mean Square(Error) = 9,09E-005.

Univariate Analysis of Variance: PTHrPA

Between-Subjects Factors

		N
Groups	1,000	4
	2,000	3
	3,000	4

Tests of Between-Subjects Effects

Dependent Variable:PTHrPA

Source	Type III Sum of Squares	df	Mean Square	F	Sig.
Corrected Model	3,008E-5[a]	2	1,504E-5	16,623	,001
Intercept	,000	1	,000	168,194	,000
Groups	3,008E-5	2	1,504E-5	16,623	,001
Error	7,238E-6	8	9,048E-7		
Total	,000	11			
Corrected Total	3,732E-5	10			

a. R Squared = ,806 (Adjusted R Squared = ,758)

Post Hoc Tests

Multiple Comparisons

PTHrPA: Tukey HSD

(I) Groups	(J) Groups	Mean Difference (I-J)	Std. Error	Sig.	95% Confidence Interval Lower Bound	95% Confidence Interval Upper Bound
1,000	2,000	-,00107	,000727	,355	-,00314	,00101
	3,000	-,00378*	,000673	,001	-,00570	-,00186
2,000	1,000	,00107	,000727	,355	-,00101	,00314
	3,000	-,00272*	,000727	,014	-,00479	-,00064
3,000	1,000	,00378*	,000673	,001	,00186	,00570
	2,000	,00272*	,000727	,014	,00064	,00479

Based on observed means.

The error term is Mean Square(Error) = 9,05E-007.

*. The mean difference is significant at the 0,05 level.